YTUP

Journal of Thermal Engineering
https://jten.yildiz.edu.tr/
https://doi.org/10.47481/jten.0080

RESEARCH ARTICLE

Investigation on the optimization of performance and emission characteristics of a VCR diesel engine fueled with Chlorella vulgaris biodiesel using Al_2O_3 and ZnO nanoparticles: a Grey-Taguchi and artificial neural network (ANN) approach

Sumit Dubal[1,*], Aryaman Salaria[2], Sahaj Joshi[3]

[1]School of Automobile Engineering, Symbiosis Skills and Professional University, Pune, 412101, India
[2]School of Automobile Engineering, Symbiosis Skills and Professional University, Pune, 412101, India
[3]School of Automobile Engineering, Symbiosis Skills and Professional University, Pune, 412101, India

Abstract

Third-generation algae biofuels, made from biomass, are a promising renewable fuel due to their low carbon footprint. In internal combustion engines, it hinders combustion and performance. This study aims to improve engine efficiency by blending algae biodiesel with nano additives. First, Grey-Taguchi optimization is used to find the best blend, compression ratio, load, EGR, and nano-additive concentration for key performance indicators. The Grey-Taguchi method efficiently analyses complex parameters and reduces experiments, saving time and resources. Following experimental data, an Artificial Neural Network (ANN) model predicted future emissions and performance. The ANN model was trained with 25 observations for 20% and 30% biodiesel blends. The ANN model predicted engine behavior with over 90% accuracy and was effective. The study shows that algae biodiesel and nano-additives can improve engine performance and provide a reliable projection method. B20CV + 100 ppm ZnO improved BTE and BP by 4.2% and 3.8% over diesel. The BSFC dropped 5.1%, showing better fuel use. However, nanoparticle agglomeration increased NOx emissions. Due to its lower calorific value, B30CV + 100 ppm ZnO reduced BTE by 6.5% and increased BSFC by 7.3%. The developed ANN model predicted performance and emissions with over 90% accuracy, with minor NOx deviations due to combustion variation. This novel study uses Grey-Taguchi optimization and ANN modelling to assess and predict engine performance and emissions from nanoparticle-enriched algae biodiesel blends.

Keywords: Algae biodiesel, nano additives, Grey-Taguchi optimization, artificial neural network (ANN), engine performance, emission reduction

Cite this article as: Dubal, S., Salaria, A., & Joshi, S. (2026). Investigation on the optimization of performance and emission characteristics of a VCR diesel engine fueled with Chlorella vulgaris biodiesel using Al_2O_3 and ZnO nanoparticles: A Grey-Taguchi and artificial neural network (ANN) approach. Journal of Thermal Engineering, 12(6), 1996–2017. https://doi.org/10.47481/jten.0080

1. Introduction

As our population growth rate has increased, our dependence on fossil fuels has surged. The major contributor to the production of greenhouse emissions is the Road Transport Industry, which produces 17% of greenhouse gases from the aggregated total [1], [2], [3] This is causing a marked intensification of climate change. Major countries are determining various forms of alternative fuels to decrease their economic dependency on each other and factors such as employment rate, environmental safety and innovation within the existing products will have a pragmatic effect [4], [5], [6]contributing to carbon emissions and accelerating climate change. It is possible to mitigate environmental damage by promoting renewable or alternative fuels, namely biofuels, solar energy, biomass, wind, geothermal, small-scale hydro, and wave power. Biofuels are considered as low carbon-emitting alternatives to conventional fuels. The use of biofuels promotes reduced emissions of greenhouse gases and reduces the related detrimental impact of transport. As an alternative to fossil fuels, renewable fuels seem to present a promising scenario. However, if low carbon products are promoted, analysis of each particular product's GHG emissions and carbon footprint (CF. The use of biodiesel as an alternative fuel is increasing because government poli-

*Corresponding Author
E-mail Adress: sdubal1585@gmail.com

Submitted: 5 January 2025; **Accepted:** 12 April 2025

This paper was recommended for publication in revised form by Editor-in-Chief Ahmet Selim Dalkılıç

cies have led many industries to adopt it. Among such fuels, internal combustion engines running on biodiesel are increasingly studied by various researchers [7], [8]. However, due to the increase in rivalry for the need for crops for human consumption and water during its cultivation process, first-generation biofuels are being staved off [9]sustainable resources of energy. For the future re-arrangement of a sustainable economy to biological raw materials, completely new approaches in research and development, production, and economy are necessary. The ‘first-generation’ biofuels appear unsustainable because of the potential stress that their production places on food commodities. For organic chemicals and materials these needs to follow a biorefinery model under environmentally sustainable conditions. Where these operate at present, their product range is largely limited to simple materials (i.e. cellulose, ethanol, and biofuels. Third-generation biofuels use crops as algae as a source of energy. Algae as biofuels were determined to be more energy-intensive than their first- and second-generation counterparts. Additionally, algae can be grown in water bodies that are unsuitable for other sources of biofuel [10].

In the past few years, most research has focused on harvesting algal biomass; for example, Nautiyal et.al carried out research to extract feedstock from Spirulina platensis algae biomass using the transesterification process. Their results showed a yield rate of biodiesel of 78% [11] Similarly Carolina carried out research where extraction of oil from Chlorella Alga by transesterification process revealed a yield of 98% [12]. Nanoparticles (NPs) have become widely famous due to their exceptional utility in various scientific disciplines [13], [14], [15], [16]. Nanomaterials, owing to their unique physicochemical properties and increased surface area, have significantly influenced material performance and are widely utilized in various automotive applications, including fuel enhancement, lubrication, and emission control [16], [17], [13], [14], [15], [18]Many studies have come to the same conclusion that nano-additives were advantageous in improving the catalytic reaction during the combustion process, which resulted in complete and rapid combustion[19], [20], [21]non-premixed diesel-air, hydrogen-air, kerosene-air, n-butanol, pentane-air, propane-air and methane–air used in a 2D geometry cylindrical combustion chamber. The numerical simulation based on the solution of the mass, momentum, energy and the chemical species conservation equations was performed for steady state condition using computation Fluid Dynamic (CFD. The research was carried out using a B20 blend of Chlorella vulgaris algal methyl ester in a four-stroke CI engine with a water-cooled system in the presence of MgO nano-additives. Their results showed that B20 (with MgO nano-additives) produced a 15.6% decrease in BSFC, a 2.5% increase in BTE, and lower HC, CO, and smoke emissions compared to B20 (without MgO nano-additives). In other experiments, Chlorella vulgaris algae biodiesel was tested in a single-cylinder, four-stroke, water-cooled engine with ZnO nanoparticles. Their results revealed similar mechanical effects between ZnO-blended biodiesel and commercial diesel. Moreover, the power was increased, and the emissions were lower due to the involvement of ZnO nano-additives when compared to only a 20% biodiesel blend [22]. However, many authors have mentioned that increased NOx emissions are being produced due to high biofuel content and hence, blending of up to 20-30% were found to be of optimum level [23]. Another study was carried out where Chlorella vulgaris in addition to Al_2O_3 was run in a single-cylinder, four-stroke CI engine. Their results showed that BSFC and BTE produced with 20% biodiesel were best with 75ppm of Al_2O_3. However, the lowest NOx emissions were obtained with 50 ppm of Al_2O_3 [24].

Various optimization techniques have been deployed in multiple applications, where an optimal combination of input parameters was determined [8]. A study was conducted in which biodiesel with various blend levels was run in a single-cylinder, four-stroke, direct-injection air-cooled engine. They determined the multi-response optimum parameters as 10% of EGR, 100% of load, and 40% using Grey-Taguchi Analysis as an optimization technique [25]. Similarly, Ramacharan et al. conducted a study in which algae biodiesel was tested in a 4-stroke, single-cylinder, water-cooled CI engine. Their results were concluded by determining the optimal microalgal energy ratio as optimization criteria using the RSM approach [26]. On the other hand, Gil. et.al used ANN to create a predicting model. By first deploying the Grey-Taguchi method, they decided the best input parameters to be B100, a speed of 2300 rpm, and 100% load. Furthermore, they used ANN to predict responses based on these parameters with an accuracy of 99.3% [27]. Out of such optimization techniques, saw from previously mentioned studies, Grey-Taguchi and ANN seemed to stand out the most [8].

In this study, we have run Chlorella Vulgaris biodiesel at 20% and 30% blend levels with an addition of Al_2O_3 and ZnO nano-additives at 50ppm and 100ppm, in a single-cylinder, four-stroke, water-cooled VCR engine. Additionally, we have used the Grey-Taguchi approach to decide the best input parameters and ANOVA to investigate the largest contributing factor to variation in the data. On the other hand, ANN was developed as a predictive model to decide responses to best input parameters. Al_2O_3 nanoparticles, due to their high thermal conductivity and catalytic activity, enhance heat transfer and facilitate complete fuel oxidation, resulting in a substantial decrease in carbon monoxide and hydrocarbon emissions and an increase in brake thermal efficiency [28], [29], [30]. Similarly, ZnO nanoparticles function as efficient combustion catalysts, enhancing fuel-air mixing and oxidation processes. This leads to enhanced engine performance and reduced emissions. Al_2O_3 and ZnO nanoparticles are effective additives for optimizing the performance and environmental impact of biodiesel-fuelled diesel engines due to these properties [31], [32], [33], [34]. Although substantial research has been conducted on algae biodiesel as a sustainable alternative fuel, multiple challenges stay unresolved. Research has shown that nano-additives improve combustion efficiency and reduce emissions. Nanoparticle agglomeration, higher NOx emissions, and engine performance variations due to biodiesel's lower calorific value remain. Earlier studies mostly used experimental analyses without systematic optimization to find the best input parameters. Grey-Taguchi optimization and ANN-based predictive modelling are used to improve biodiesel performance and reduce experiments. This research fills it. Our approach systematically decides the best blend level, compression ratio, engine load, EGR rate, and nano-additive concentration, making it more comprehensive and scalable than earlier studies that focused on individual biodiesel blends or nano-additives. The ANN model is a significant improvement over traditional trial-and-error methods providing a predictive tool with over 90% accuracy and thereby extending the study's applicability. This novel approach promises enhanced engine performance, improved emissions control, and a more efficient method for future research on biodiesel applications.

2. Materials and methods

2.1. Synthesis of biodiesel

Chlorella vulgaris algal oil was sourced externally to produce our required biodiesel blends by the transesterification process. Figure 1 shows the algae in its first form and the oil extracted from the algae at the final stage of transesterification. The nano-additives were provided by the facility where we performed our experiments. Table 4 lists the fuel blends that we synthesized for our experiment. Moreover, various chemical tests were performed, by the standards, to decide the chemical properties of our blends Table 5 presents the physical and chemical properties of various biodiesel blends.

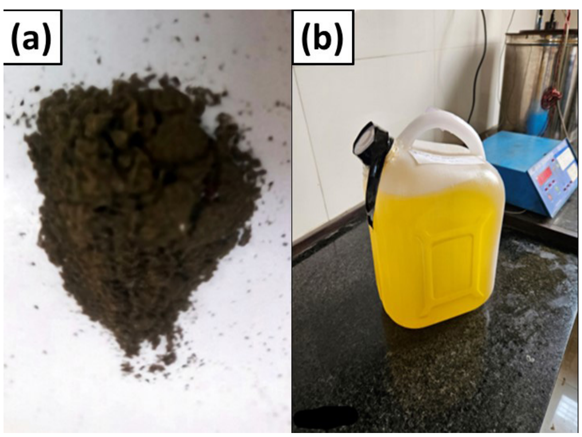

Figure 1. a) Chlorella Vulgaris biomass powder, **b)** Algae biodiesel

2.2 Experiment setup

The study was conducted on a single-cylinder, four-stroke naturally aspirated water-cooled engine that had a variable compression ratio. The engine load was applied haphazardly using the eddy current dynamometer. The exhaust emissions produced by the engine were measured using the AVL-437 smoke meter in conjunction with the AVL Digas 444N EGR. To analyses the performance and combustion variables of the engine, a piezoresistive transducer in the cylinder head and a crank angle sensor were used. The results were promptly displayed on the computer that was directly connected to a high-speed data acquisition system. Table 1 depicts engine specifications.

Table 1. Engine specifications

Make	**Kirloskar**
Engine Cycle	4-stroke
Rated Speed	1500 rpm
Rated Power	3.5 kilowatts
Type of Dynamometer	Eddy current dynamometer
Bore Diameter	87.5 millimeters
Stroke Length	110 millimeters
Cooling System	Water cooled
Cubic Capacity	661 liters (661 cc)
Ignition System	Compression-Ignition
Compression Ratio	12-18

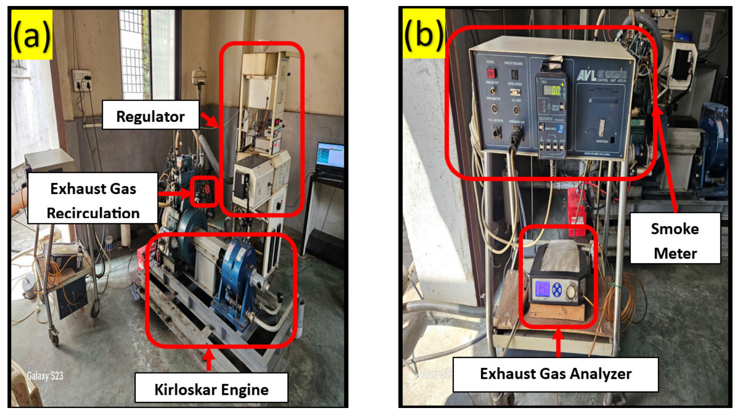

Figure 2. a) Kirloskar 4-stroke engine with exhaust gas recirculation, **b)** Exhaust Gas analyzer and smoke meter

Tables 2 and 3 depict the specifications of the AVL DIGAS 444N Gas Analyzer and the AVL Smoke Meter, respectively.

Table 2. AVL DIGAS 444N Gas analyzer specifications

Model Name/Number	**AVL DIGAS 444N Gas Analyzer**
Application	For Petrol, CNG and Gas Vehicle Pollution Check
Analysis Time	2 min
Automation Grade	Automatic
Display Type	Digital
Response Time	2 min
Weight	6 Kg
Measurement Principle	Filter Paper Blackening
Resolution Ratio	0.001 FSN or 0.01 mg/m^3
Warm Up	5 min
Detection Limit	0.002 FSN or 0.02 mg/m^3
Measured value output	FSN (filter smoke number), mg/m^3 (soot concentration)
Measurement Range	0-10 FSN

Table 3. AVL Smoke meter specifications

Model Name	AVL Smoke Meter
Measurement principle	Filter paper blackening
Measured value output	FSN (filter smoke number), mg/m³ (soot concentration)
Measurement range	0 to 10 FSN
Detection limit	0.002 FSN or 0.02 mg/m³

2.3. Experiment procedure

Initially, the required fuel was introduced into the fuel tank of the setup. Furthermore, lubricating oil and water levels were checked, and the eddy-current dynamometer was calibrated to prevent loading errors. Additionally, the CR of the engine was varied accordingly, and once the engine started, input parameters such as load and EGR were manually adjusted using regulators. The variation in input parameters, such as injection pressure and injection timing of the engine, was achievable because of its steady-state conditions, and various exhaust-gas-emission instruments were connected to the tailpipe. Figure 2 shows the engine setup used in our experiment. The gas analyzer and smoke meter were ARAI-calibrated for emissions. After checking the power supply, electrical calibration, and accessory functionality, the gas analyzer was span- and zero-calibrated for CO and HC measurements using suitable sample gas. The sampling system, printer, and digital display were leak-checked and calibrated before an idling emission test. Smoke meter calibration used neutral-density filter paper, oil-temperature and RPM sensors, optical-chamber heating, and purge-air systems to check zero- and mid-scale points. Electrical earthing continued. Visual displays, internal components, and sample hose were checked. Finally, a free acceleration test verified instrument performance.

2.4. Taguchi optimization techniques

The Taguchi optimization technique is an analytical method introduced by Dr. Genichi Taguchi. Its aim is to minimize procedural variation by producing a well-defined set of experiments. A distinctive set of orthogonal matrices or arrays is produced which reduces the number of experiments that need to be performed. Furthermore, the layout of the orthogonal matrix is constructed using sequential control variables and the number of degrees assigned to each variable. A statistical approximation known as SNR, or signal-to-noise ratio, is used in Taguchi optimization. It is the dispersion around the ideal value. Taguchi categorized the SNR into three categories: larger-is-better, smaller-is-better, and nominal-is-better. If the variable needs to be minimized smaller-is-better values are calculated using equation (1). On the other hand, if the variable is required to be maximized, then larger-is-better values are calculated using equation (2) [25], [35], [36].

Table 4. Various blends used in our experiment

Sr. no	Diesel Volume (%)	C.Vulgaris Volume (%)	Nano-additives (ppm)		Fuel Blends
			Al_2O_3	ZnO	
1	80	20	0	0	B20CV
2	80	20	50	0	B20CV + 50ppm Al_2O_3
3	80	20	100	0	B20CV + 100ppm Al_2O_3
4	80	20	0	50	B20CV + 50ppm ZnO
5	80	20	0	100	B20CV + 100ppm ZnO
6	70	30	0	0	B30CV
7	70	30	50	0	B30CV + 50ppm Al_2O_3
8	70	30	100	0	B30CV + 100ppm Al_2O_3
9	70	30	0	50	B30CV + 50ppm ZnO
10	70	30	0	100	B30CV + 100ppm ZnO

Table 5. Physical and chemical properties of various nature of fuel

Properties	Unit	ASTM Method	Std Diesel	B20CV	B20CV + 50PPM Al_2O_3	B20CV + 100PPM Al_2O_3	B30CV + 50PPM ZnO	B30CV + 100PPM ZnO
Density	Kg/m3	D287	816	833	835	837	836	839
Calorific Value	kj/kg	D4809	42851.9	40562	41315.3	41411.6	40570.1	41010
Flash Point	°C	D9358T	53	68	66	72	69	73
Fire Point	°C	D9358T	56	72	68	74	71	74
Kinematic Viscosity	cST	D445	2.09	2.31	2.08	2.21	2.43	2.58

Table 6. Input parameters with level of variations (B20)

Control Variables	Levels L-1	L-2	L-3	L-4	L-5
Blend	B20CV	B20CV+50ppm Al_2O_3	B20CV+100ppm Al_2O_3	B20CV+50ppm ZnO	B20CV+100ppm ZnO
Compression Ratio	14	15	16	17	18
Injection pressure (MPa)	20	30	40	50	60
Injection timing (° before TDC)	17	19	21	23	25
Load (%)	0	25	50	75	100
EGR (%)	0	3	6	9	12

Table 7. Input parameters with level of variations (B30)

Control Variables	Levels L-1	L-2	L-3	L-4	L-5
Blend	B30CV	B30CV+50ppm Al_2O_3	B30CV+100ppm Al_2O_3	B30CV+50ppm ZnO	B30CV+100ppm ZnO
Compression Ratio	14	15	16	17	18
Injection pressure (MPa)	20	30	40	50	60
Injection timing (° before TDC)	17	19	21	23	25
Load (%)	0	25	50	75	100
EGR (%)	0	3	6	9	12

$$SNR_S = -10\log\left(\frac{1}{n}\sum_{i=1}^{n} Yi^2\right) \tag{1}$$

$$SNR_L = -10\log\left(\frac{1}{n}\sum_{i=1}^{n}\frac{1}{Y_i^2}\right) \tag{2}$$

In this experiment, the larger-is-better SNR criterion was applied to the following output variables: BTE, BMEP, and BP. Conversely, the smaller is better SNR was used for the variable BSFC and other emission parameters such as NO_x, CO, HC, CO_2, O_2 and Smoke. Tables 6 and 7 show the variable levels and their values for the 20% and 30% biodiesel blends, respectively.

2.5. Grey-relational analysis

Considering that our experiment deals with multi-objective optimization of multiple response variables, Grey-relational analysis seems to be the most qualified statistical approach to determine the most important factors of the experiment and their relationship with each other [37]The procedure involves three steps: first, normally SNR values are decided using Taguchi; second, their deviation sequence is calculated; and third, GRG values are decided by averaging GRC values. This methodology converts a multi-variable optimization problem into a single-variable optimization problem [38].

Stage 1: Normalized values obtained from the SNR range from 0 to 1, and, according to the nature of the response, the method for deciding these normalized values is categorized into two parts: better. For variables such as BTE, BP and BMEP, the higher-is-better normalized values are calculated using equation (3). For variables such as BSFC and emission norms such as NO_x, CO, HC, CO_2, O_2, and Smoke, the smaller-is-better normalized values are calculated using equation(4) [39].

$$x_{ij} = \frac{y_{ij} - \min(y_{ij})}{\max(y_{ij}) - \min(y_{ij})} \tag{3}$$

$$x_{ij} = \frac{\max(y_{ij}) - y_{ij}}{\max(y_{ij}) - \min(y_{ij})} \tag{4}$$

where, x_{ij} is the normalized SNR, y_{ij} is the SNR obtained from Taguchi analysis, min (y_{ij}) and max y_{ij}) are minimum and largest SNR respectively.

Stage 2: The deviation sequence of the normalized values measures how far a system's characteristic deviates from its standard or desired behavior. It is the difference between the value being compared and the reference value across a series of points. Equation (5) is used to calculate the deviation sequence of the normalized SNR [40].

$$\Delta_i(k) = |\, x_0(k) - x_i(k)| \tag{5}$$

where, $\Delta_i(k)$ is the deviation sequence of normalized SNR, $x_0(k)$ is the ideal sequence and $x_i(k)$ is the given sequence.

Stage 3: The Grey-relational grades (GRGs)are calculated as the means of Grey-relational coefficients (GRCs). The GRCs indicate to us the relationship between ideal outputs and actual experimental results. It is calculated by using equation (6) [39].

$$\xi_i(k) = \frac{\Delta_{min}(\Delta_i(k)) + \psi\Delta_{max}(\Delta_i(k))}{\Delta_i(k) + \psi\Delta_{max}(\Delta_i(k))} \tag{6}$$

where, $\xi_i(k)$ is the Grey-relational coefficient, $\Delta_{min}(\Delta_i(k))$ and $\Delta_{max}(\Delta_i(k))$ are the minimum and maximum values of the deviation sequence, $\Delta_i(k)$ is the actual reference value of the deviation sequence and is known as the distinguishing coefficient that varies between $0<\psi<1$.

2.6. Analysis of variance (ANOVA)

ANOVA is a statistical method for deciding the factor that contributes the largest percentage of variance in the data. This approach was implemented using MATLAB R2024a (24.1) Moreover, input variables with greater F-values have a greater effect on the response variables.

2.7. ANN modelling

An artificial neural network (ANN) is a type of artificial intelligence that can recognize complex patterns and make predictions of future output variables [41]. It models itself after a human brain's architecture and functionality [42]. An ANN model consists of nodes or neurons, each of which is a simple processing unit. A conventional structure of the ANN model is arranged in an advanced manner, starting with an input layer, then a hidden layer and at last the output layer [43]. Figure 3 shows the architecture of the ANN model that we created using the 'Neural Network Fitting' tool in MATLAB R2024a (24.1).

3. Results and discussions

3.1. Taguchi optimization results

In this analysis, an L25 orthogonal array (OA) of the Taguchi method was used to decide the best engine load, compression ratio, injection pressure, injection timing, and exhaust-gas recirculation in a diesel engine powered by a C. vulgaris algal biodiesel blend. Table 8 and Table 9 show the combinations of input parameters in the L25 OA for the B20 and B30 blend levels, respectively. The responses that we obtained were categorized into two groups: better. Variables that needed to be maximized were BTE, BMEP, and BP; hence, their SNRs were considered as larger-the-better. Simultaneously, variables that needed to be minimized were BSFC and emission parameters like NOx, CO, HC, CO_2, O_2 and Smoke and their SNR were considered as smaller the better. After measuring the SNR at five levels of a particular factor, the results were collected in Tables 10 and 11 for the B20 and B30 blend levels respectively.

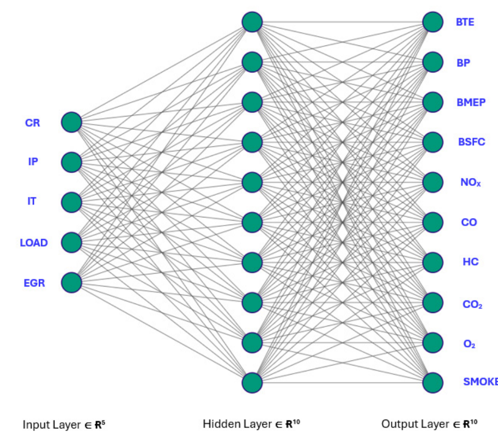

Figure 3. Artificial neural network architecture

Table 8. L25 Orthogonal array (B20)

EXP NO.	Blend Name	BLEND CODE	CR	IP (MPa)	IT (0b TDC)	LOAD (%)	EGR (%)
1		A1	14	20	17	0	0
2		A2	15	30	19	25	3
3	B20CV+50 ppm Al_2O_3	A3	16	40	21	50	6
4		A4	17	50	23	75	9
5		A5	18	60	25	100	12
6		A6	14	30	21	75	12
7		A7	15	40	23	100	0
8	B20CV+100 ppm Al_2O_3	A8	16	50	25	0	3
9		A9	17	60	17	25	6
10		A10	18	20	19	50	9
11		A11	14	40	25	25	9
12		A12	15	50	17	50	12
13	B20CV+50 ppm ZnO	A13	16	60	19	75	0
14		A14	17	20	21	100	3
15		A15	18	30	23	0	6
16		A16	14	50	19	100	6
17		A17	15	60	21	0	9
18	B20CV+100 ppm ZnO	A18	16	20	23	25	12
19		A19	17	30	25	50	0
20		A20	18	40	17	75	3
21		A21	14	60	23	50	3
22		A22	15	20	25	75	6
23	B20	A23	16	30	17	100	9
24		A24	17	40	19	0	12
25		A25	18	50	21	25	0

Table 9. L25 orthogonal array (B30)

EXP NO.	Blend Name	Blend Code	CR	IP (MPa)	IT (0b TDC)	LOAD (%)	EGR (%)
1	B30CV+50 ppm Al_2O_3 LCV: 40980 Density: 834	B1	14	20	17	0	0
2		B2	15	30	19	25	3
3		B3	16	40	21	50	6
4		B4	17	50	23	75	9
5		B5	18	60	25	100	12
6	B30CV+100 ppm Al_2O_3 LCV: 41052 Density: 838	B6	14	30	21	75	12
7		B7	15	40	23	100	0
8		B8	16	50	25	0	3
9		B9	17	60	17	25	6
10		B10	18	20	19	50	9
11	B30CV+50 ppm ZnO LCV: 40901 Density: 834	B11	14	40	25	25	9
12		B12	15	50	17	50	12
13		B13	16	60	19	75	0
14		B14	17	20	21	100	3
15		B15	18	30	23	0	6
16	B30CV+100 ppm ZnO LCV: 40955 Density: 836	B16	14	50	19	100	6
17		B17	15	60	21	0	9
18		B18	16	20	23	25	12
19		B19	17	30	25	50	0
20		B20	18	40	17	75	3
21	B30CV LCV: 40151 Density: 845	B21	14	60	23	50	3
22		B22	15	20	25	75	6
23		B23	16	30	17	100	9
24		B24	17	40	19	0	12
25		B25	18	50	21	25	0

Table 10. SNR for B20

	Larger-the-Better			Smaller-the-Better						
Run	**BTE**	**BMEP**	**BP**	**BSFC**	**NOx**	**CO**	**HC**	**CO2**	**O2**	**Smoke**
1	8.81	-26.02	-0.44	13.99	-25.11	12.40	-42.86	-6.02	-24.98	-29.25
2	20.59	-20.00	-0.92	1.72	-35.42	8.18	-41.58	-13.80	-22.78	-13.98
3	26.02	-13.56	4.61	7.13	-42.14	17.08	-26.85	-8.94	-24.68	-16.39
4	26.61	-10.17	8.30	7.74	-44.40	12.04	-30.10	-11.82	-23.80	-24.19
5	25.01	-8.40	9.54	6.20	-44.96	-6.65	-42.80	-17.38	-19.49	-30.32
6	23.11	-10.17	7.60	4.29	-39.55	-13.98	-50.71	-19.55	-11.41	-25.20
7	26.89	-7.74	10.37	7.96	-51.78	7.74	-36.39	-15.12	-22.32	-32.93
8	-0.65	-29.12	-6.88	18.61	-22.28	7.54	-40.26	-6.02	-24.92	-12.87
9	22.67	-20.00	-0.92	3.88	-38.89	13.98	-29.25	-9.83	-24.35	-8.63
10	26.02	-13.56	4.61	7.13	-45.15	15.92	-24.61	-12.26	-23.68	-22.80
11	20.75	-20.00	-0.92	1.72	-27.23	8.40	-41.87	-13.06	-23.08	-12.87
12	23.23	-13.56	4.61	4.29	-35.99	-1.80	-43.75	-18.17	-18.90	-9.25
13	26.15	-11.06	7.23	7.13	-48.88	21.94	-22.28	-7.60	-24.81	-11.60
14	26.49	-7.74	10.10	7.54	-47.04	1.72	-37.15	-15.99	-21.51	-23.52
15	4.77	-32.77	-4.38	10.43	-27.60	12.04	-28.63	-6.02	-25.12	-2.92
16	25.58	-7.74	10.37	6.74	-43.11	-7.57	-46.65	-17.84	-18.92	-30.58
17	-14.73	-10.96	2.79	15.07	-20.83	6.74	-45.48	-9.25	-24.30	-18.69
18	20.09	-20.00	-1.94	1.21	-26.85	3.61	-43.52	-14.96	-22.15	-7.23
19	24.45	-15.39	2.92	5.51	-42.92	26.02	-21.58	-2.92	-25.58	-16.65
20	27.04	-10.17	8.30	8.18	-52.71	18.42	-25.11	-12.46	-23.63	-18.28
21	25.11	-13.56	4.61	6.20	-43.29	17.08	-30.10	-8.30	-24.75	-2.92
22	26.24	-10.17	7.60	7.33	-42.08	6.20	-38.59	-16.26	-21.45	-15.85
23	24.71	-8.40	9.25	5.68	-43.11	-8.97	-46.49	-18.59	-17.28	6.02
24	13.69	-17.65	-12.14	4.95	-18.06	13.15	-30.37	-4.61	-25.34	7.96
25	22.86	-20.00	-0.92	3.88	-41.06	20.00	-27.23	-4.61	-25.40	-16.39

Table 11. SNR for B30

	Larger-the-Better			Smaller-the-Better						
Run	**BTE**	**BMEP**	**BP**	**BSFC**	**NOx**	**CO**	**HC**	**CO2**	**O2**	**Smoke**
1	13.79	-20.00	2.32	-2.34	-19.08	8.87	-47.42	-8.63	-24.40	-35.65
2	21.29	-20.00	-0.92	2.38	-34.49	10.17	-38.99	-12.04	-23.58	-9.25
3	24.51	-15.39	2.92	5.68	-43.81	1.83	-28.63	-12.46	-23.56	4.44
4	26.69	-10.17	8.30	7.74	-48.53	9.63	-34.15	-14.96	-22.33	-10.88
5	24.19	-8.40	9.25	5.35	-40.17	-11.95	-48.16	-18.89	-15.07	-26.97
6	23.52	-10.17	7.60	4.58	-36.39	-13.37	-49.57	-19.08	-13.80	-26.73
7	26.57	-7.74	10.37	7.74	-48.27	8.18	-36.78	-12.46	-23.63	-32.91
8	22.22	-24.44	8.03	12.77	0	-24.71	-7.23	-42.61	6.94	-16.12
9	21.94	-20.00	-0.92	3.10	-35.99	11.37	-33.80	-12.26	-23.59	-12.87
10	25.48	-13.56	4.61	6.56	-45.67	11.70	-33.62	-15.12	-22.27	-24.30
11	20.67	-20.00	-0.92	1.83	-34.96	8.40	-42.01	-12.87	-23.29	-25.71
12	21.94	-13.56	4.61	2.97	-34.96	-10.50	-50.24	-19.82	-14.01	-16.65
13	27.12	-10.17	8.30	8.18	-52.65	17.72	-30.63	-12.26	-23.76	-18.28
14	27.08	-7.74	10.10	8.18	-47.99	2.38	-38.89	-16.12	-21.45	-29.97
15	16.71	-40.00	-8.97	4.85	-27.60	10.17	-30.10	-6.02	-25.10	-2.28
16	27.27	-7.74	10.37	8.40	-51.89	0.00	-43.75	-17.38	-20.21	-35.50
17	12.72	-23.10	-3.03	-0.06	-16.90	6.56	-45.89	-8.94	-24.34	-28.33
18	19.55	-20.00	-1.94	0.63	-27.23	4.58	-43.69	-14.29	-22.49	-19.28
19	25.53	-13.56	4.61	6.56	-50.40	16.48	-31.13	-11.36	-23.90	-18.89
20	27.08	-10.17	8.30	8.18	-53.61	16.48	-30.88	-13.06	-23.38	-23.75
21	26.15	-13.56	4.61	7.13	-45.98	1.83	-34.96	-10.88	-23.97	-18.79
22	26.19	-10.17	7.60	7.13	-41.66	4.88	-40.34	-17.15	-20.53	-18.99
23	24.35	-8.40	9.25	5.35	-40.91	-11.20	-48.37	-25.48	-15.45	-26.19
24	14.33	-24.44	-5.63	3.92	-20.83	8.87	-39.65	-8.63	-24.46	7.96
25	22.08	-20.00	-0.92	2.97	-42.86	19.17	-25.11	-6.44	-25.16	-2.92

3.2. Interpretation of values using GRA

The Taguchi optimization technique previously mentioned can only be used for single-objective optimization, which means that different best settings are seen for each variable. This introduced a new complication into our analysis. To solve such complications, the Grey-Relational Analysis complements Taguchi was utilized because it deals with the multi-objective optimization of multi-response variables [44].

First and foremost, the SNRs obtained for various factors were normalized using equations 3 and 4. Once again, were categorized as larger-the-better or smaller-the-better. Tables 12 and 13 present the normalized SNR values for B20 and B30 blend levels, respectively. Deviation sequences for each normalized SNR were calculated using Equation 5 and are presented in Tables 14 and 15. This helped us decide the GRC values using equation 6, as shown in Tables 16 and 17.

Using Grey-Taguchi for B20 and B30 blend levels of biodiesel showed that Experiment No. 16 (B20 + 100ppm ZnO and B30 + 100ppm ZnO), with 14 CR, 500 MPa IP, 19°b TDC of IT at 100% engine load and 6% EGR, produced best results. This is because they obtained the highest grey-relation grade in the experiment. Once the GRG values for each experiment were decided, the SNR curve of GRG against all input parameters was produced. Figures 3 and 4 show the SNR curves for GRG Vs Blend, CR, IP, IT, Load, and EGR for the B20 and B30 fuel blend levels, respectively. Note that the GRG values were considered as larger-the-better.

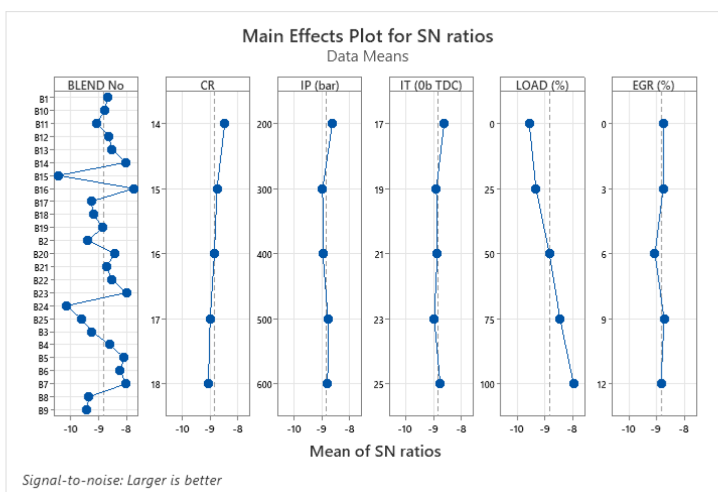

Figure 4. B20 best combination of parameters

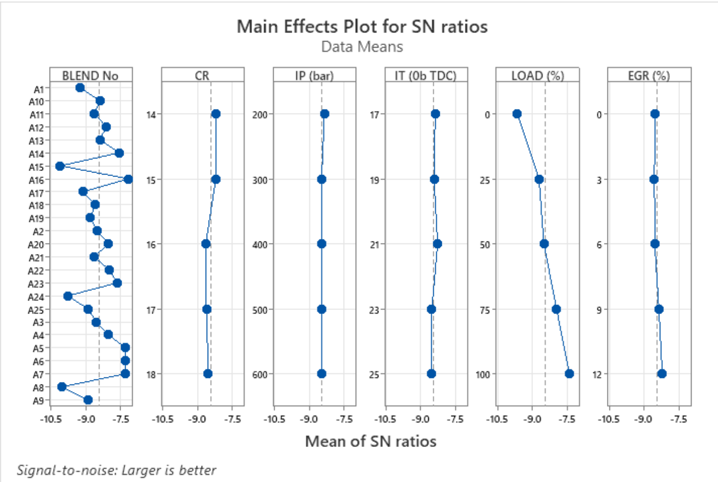

Figure 5. B30 best combination of parameters

The results showed that the best combination of parameters was B20 + 100ppm ZnO with CR of 14, IP of 200MPa, and IT of 21°b TDC when the engine load was 100% and the EGR level was 12%. Moreover, at the B30 blend level, the best combination of parameters produced was B30 + 100ppm ZnO with CR of 14, IP of 200MPa, and IT of 17° b TDC at 100% engine load and 9% EGR.

3.3 Analysis of variance (ANOVA)results

Analysis of variance was performed using MINITAB21 (21.4.2), a statistical software package. This estimates the percentage contribution of variance of data for each input factor and translates the most effective and significant input factor of the optimal combination [45]. The results obtained from the ANOVA model for the B20, and B30 blends are presented in Tables 18 and 19, respectively. For both blends, the load was the largest contributing factor to the variance in the data. For the B20 blend, the load contributed 87.9% and had an F-value of 45.99. On the other hand, for the B30 blend, the load contributed 78.73% and had an F-value of 30.12.

3.4 Assessed and simulated ANN result

The final step in interpreting our results is to decide the performance and emission parameters associated with the best input parameters obtained through Grey-Taguchi Analysis and to compare these parameters with those simulated using the ANN technique. The ANN model, developed in MATLAB, is a feed-forward back propagation network with three layers of neural [46]. The first layer is the input layer, which consists of 5 (LOGSIG) neurons; the second layer is the hidden layer, which consists of 10 (LOGSIG) neurons; and the final layer is the output layer, which consists of 10 (PURLINE) neurons. The experiment was performed using the best input data, decided by trial and error, until the mean square difference between the experimental data and the predicted response was minimized. A training function known as "Trainlm" was used to train the ANN model, Moreover, the optimization algorithm used was "Levenberg-Marquardt". Once the model was created, its performance was evaluated and regression analysis was conducted. Illustrations of the analysis are presented in Figures 6 and 7. Figures 6c-6d and 7c-7d show the performance and regression results obtained by the ANN models for the B20 and B30 blends, respectively. Since the regression values of both models are very close to 1, the results predicted by the ANN model can be considered satisfactory. A common way to train artificial neural networks (ANNs) is to use the Levenberg-Marquardt (LM) algorithm. This is particularly effective when the network is trained with examples (supervised learning). It improves performance by adjusting the network's settings (weights) while it's being trained. It uses both gradient descent (which moves in the direction that reduces errors) and the Gauss-Newton method (which examines how errors change with the network configuration) in its formulation. When these methods are used together, the LM algorithm minimizes errors more effectively, which is the primary aim in training an ANN.

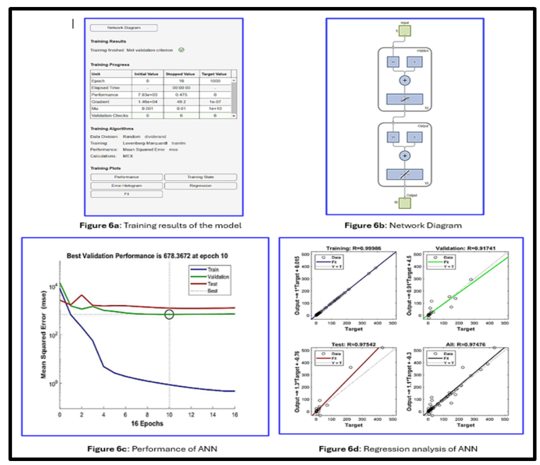

Figure 6. Illustrations of ANN model (B20 Blend)

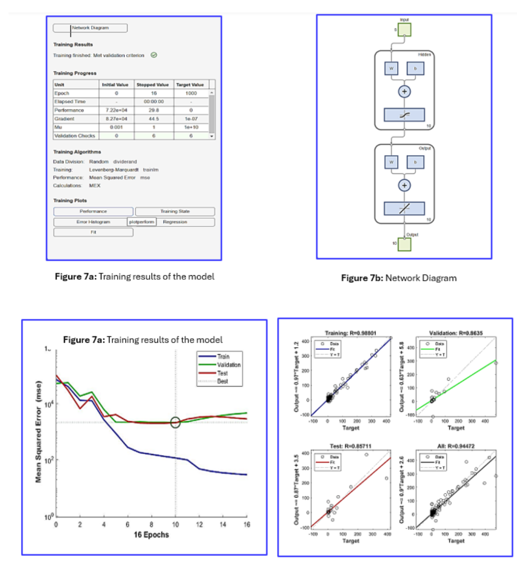

Figure 7. Illustrations of ANN model (B30 Blend)

3.5. Comparison of results

Through Grey-Taguchi analysis, we found that 100ppm ZnO as a nano-additive in both 20% and 30% biodiesel blends are best. To confirm the GRA and ANN results, a confirmation test was carried out under conditions defined by the best combination of input parameters determined through Grey-Taguchi. Tables 20 and 21 include the parameters on which B20CV + 100ppm ZnO and B30CV + 100ppm ZnO were run, respectively, in the same experimental setup.

3.5.1. Comparison of B20CV algae biodiesel against standard diesel

3.5.1.1. Brake thermal efficiency (BTE)

BTE measures the efficiency with which an engine converts the chemical energy of fuel into mechanical energy. Figure 8a compares the BTE of B20CV + 100 ppm ZnO with that of standard diesel. The higher BTE of biodiesel may result from enhanced combustion efficiency and improved fuel atomization, with ZnO nanoparticles acting as catalysts and thereby improving combustion.

3.5.1.2. Brake power (BP)

BP measures the engine's actual mechanical power output. Figure 8b shows that B20CV + 100 ppm ZnO outperforms standard diesel, likely due to biodiesel's oxygen-rich content, which promotes more complete and favorable combustion.

3.5.1.3. Brake means effective pressure (BMEP)

Figure 8c compares BMEP for B20CV + 100 ppm ZnO and standard diesel, showing similar values. BMEP measures the average pressure in the combustion chamber; similar energy densities of the fuels might explain why BMEP remained unchanged.

3.5.1.4. Brake specific fuel consumption (BSFC)

The BSFC is the fuel consumed per unit of power output. The BSFC for B20CV + 100 ppm ZnO is lower than that for regular diesel (Figure 8d). This is likely because ZnO nanoparticles increase the combustion temperature and accelerate reactions, as described by the Arrhenius equation. Equation 7.

As the temperature T increases the exponential term becomes larger, leading to an increase in the reaction rate constant K. This means that the chemical reactions go ahead more quickly at higher temperatures. On the other hand, the lower volatility of biodiesel compared to standard diesel leads to a more controlled and complete combustion process, hence improving combusti.

Table 12. Normalized values of B20 fuel blend

	Larger-the-Better			Smaller-the-Better						
Run	**BTE**	**BMEP**	**BP**	**BSFC**	**NOx**	**CO**	**HC**	**CO2**	**O2**	**Smoke**
1	0.56	0.26	0.52	0.27	0.20	0.34	0.73	0.19	0.96	0.91
2	0.85	0.51	0.50	0.97	0.50	0.45	0.69	0.65	0.80	0.54
3	0.98	0.77	0.74	0.66	0.70	0.22	0.18	0.36	0.94	0.60
4	0.99	0.90	0.91	0.62	0.76	0.35	0.29	0.54	0.87	0.79
5	0.95	0.97	0.96	0.71	0.78	0.82	0.73	0.87	0.57	0.94
6	0.91	0.90	0.88	0.82	0.62	1.00	1.00	1.00	0.00	0.81
7	1.00	1.00	1.00	0.61	0.97	0.46	0.51	0.73	0.77	1.00
8	0.34	0.14	0.23	0.00	0.12	0.46	0.64	0.19	0.95	0.51
9	0.90	0.51	0.50	0.85	0.60	0.30	0.26	0.42	0.91	0.41
10	0.98	0.77	0.74	0.66	0.78	0.25	0.10	0.56	0.87	0.75
11	0.85	0.51	0.50	0.97	0.26	0.44	0.70	0.61	0.82	0.51
12	0.91	0.77	0.74	0.82	0.52	0.70	0.76	0.92	0.53	0.42
13	0.98	0.87	0.86	0.66	0.89	0.10	0.02	0.28	0.95	0.48
14	0.99	1.00	0.99	0.64	0.84	0.61	0.53	0.79	0.71	0.77
15	0.47	0.00	0.34	0.47	0.28	0.35	0.24	0.19	0.97	0.27
16	0.96	1.00	1.00	0.68	0.72	0.84	0.86	0.90	0.53	0.94
17	0.00	0.87	0.66	0.20	0.08	0.48	0.82	0.38	0.91	0.65
18	0.83	0.51	0.45	1.00	0.25	0.56	0.75	0.72	0.76	0.37
19	0.94	0.69	0.67	0.75	0.72	0.00	0.00	0.00	1.00	0.60
20	1.00	0.90	0.91	0.60	1.00	0.19	0.12	0.57	0.86	0.64
21	0.95	0.77	0.74	0.71	0.73	0.22	0.29	0.32	0.94	0.27
22	0.98	0.90	0.88	0.65	0.69	0.50	0.58	0.80	0.71	0.58
23	0.94	0.97	0.95	0.74	0.72	0.87	0.86	0.94	0.41	0.05
24	0.68	0.60	0.00	0.79	0.00	0.32	0.30	0.10	0.98	0.00
25	0.90	0.51	0.50	0.85	0.66	0.15	0.19	0.10	0.99	0.60

Table 13. Normalized values of B30 fuel blend

	Larger-the-Better			Smaller-the-Better						
Run	**BTE**	**BMEP**	**BP**	**BSFC**	**NOx**	**CO**	**HC**	**CO2**	**O2**	**Smoke**
1	0.07	0.62	0.58	1.00	0.06	0.23	0.93	0.07	0.98	1.00
2	0.59	0.62	0.42	0.69	0.48	0.21	0.74	0.16	0.95	0.39
3	0.81	0.76	0.61	0.47	0.73	0.40	0.50	0.18	0.95	0.08
4	0.96	0.92	0.89	0.33	0.86	0.22	0.63	0.24	0.91	0.43
5	0.79	0.98	0.94	0.49	0.63	0.71	0.95	0.35	0.69	0.80
6	0.74	0.92	0.86	0.54	0.53	0.74	0.98	0.36	0.65	0.80
7	0.95	1.00	1.00	0.33	0.85	0.25	0.69	0.18	0.95	0.94
8	0.65	0.48	0.88	0.00	-0.46	1.00	0.00	1.00	0.00	0.55
9	0.63	0.62	0.42	0.64	0.52	0.18	0.62	0.17	0.95	0.48
10	0.88	0.82	0.70	0.41	0.78	0.17	0.61	0.25	0.91	0.74
11	0.55	0.62	0.42	0.72	0.49	0.25	0.81	0.19	0.94	0.77
12	0.63	0.82	0.70	0.65	0.49	0.68	1.00	0.38	0.65	0.56
13	0.99	0.92	0.89	0.30	0.97	0.03	0.54	0.17	0.96	0.60
14	0.99	1.00	0.99	0.30	0.85	0.38	0.74	0.28	0.88	0.87
15	0.27	0.00	0.00	0.52	0.29	0.21	0.53	0.00	1.00	0.23
16	1.00	1.00	1.00	0.29	0.95	0.44	0.85	0.31	0.85	1.00
17	0.00	0.52	0.31	0.85	0.00	0.29	0.90	0.08	0.97	0.83
18	0.47	0.62	0.36	0.80	0.28	0.33	0.85	0.23	0.92	0.62
19	0.88	0.82	0.70	0.41	0.91	0.06	0.56	0.15	0.96	0.62
20	0.99	0.92	0.89	0.30	1.00	0.06	0.55	0.19	0.94	0.73
21	0.92	0.82	0.70	0.37	0.79	0.40	0.64	0.13	0.96	0.61
22	0.93	0.92	0.86	0.37	0.67	0.33	0.77	0.30	0.86	0.62
23	0.80	0.98	0.94	0.49	0.65	0.69	0.96	0.53	0.70	0.78
24	0.11	0.48	0.17	0.59	0.11	0.23	0.75	0.07	0.98	0.00
25	0.64	0.62	0.42	0.65	0.71	0.00	0.42	0.01	1.00	0.25

Table 14. Deviation sequence of B20 blend fuel

Run	**BTE**	**BMEP**	**BP**	**BSFC**	**NOx**	**CO**	**HC**	**CO_2**	**O_2**	**Smoke**
1	0.44	0.74	0.48	0.73	0.80	0.66	0.27	0.81	0.04	0.09
2	0.15	0.49	0.50	0.03	0.50	0.55	0.31	0.35	0.20	0.46
3	0.02	0.23	0.26	0.34	0.30	0.78	0.82	0.64	0.06	0.40
4	0.01	0.10	0.09	0.38	0.24	0.65	0.71	0.46	0.13	0.21
5	0.05	0.03	0.04	0.29	0.22	0.18	0.27	0.13	0.43	0.06
6	0.09	0.10	0.12	0.18	0.38	0.00	0.00	0.00	1.00	0.19
7	0.00	0.00	0.00	0.39	0.03	0.54	0.49	0.27	0.23	0.00
8	0.66	0.86	0.77	1.00	0.88	0.54	0.36	0.81	0.05	0.49
9	0.10	0.49	0.50	0.15	0.40	0.70	0.74	0.58	0.09	0.59
10	0.02	0.23	0.26	0.34	0.22	0.75	0.90	0.44	0.13	0.25
11	0.15	0.49	0.50	0.03	0.74	0.56	0.30	0.39	0.18	0.49
12	0.09	0.23	0.26	0.18	0.48	0.30	0.24	0.08	0.47	0.58
13	0.02	0.13	0.14	0.34	0.11	0.90	0.98	0.72	0.05	0.52
14	0.01	0.00	0.01	0.36	0.16	0.39	0.47	0.21	0.29	0.23
15	0.53	1.00	0.66	0.53	0.72	0.65	0.76	0.81	0.03	0.73
16	0.04	0.00	0.00	0.32	0.28	0.16	0.14	0.10	0.47	0.06
17	1.00	0.13	0.34	0.80	0.92	0.52	0.18	0.62	0.09	0.35
18	0.17	0.49	0.55	0.00	0.75	0.44	0.25	0.28	0.24	0.63
19	0.06	0.31	0.33	0.25	0.28	1.00	1.00	1.00	0.00	0.40
20	0.00	0.10	0.09	0.40	0.00	0.81	0.88	0.43	0.14	0.36
21	0.05	0.23	0.26	0.29	0.27	0.78	0.71	0.68	0.06	0.73
22	0.02	0.10	0.12	0.35	0.31	0.50	0.42	0.20	0.29	0.42
23	0.06	0.03	0.05	0.26	0.28	0.13	0.14	0.06	0.59	0.95
24	0.32	0.40	1.00	0.21	1.00	0.68	0.70	0.90	0.02	1.00
25	0.10	0.49	0.50	0.15	0.34	0.85	0.81	0.90	0.01	0.40

Table 15. Deviation sequence of B30 blend fuel

Run	BTE	BMEP	BP	BSFC	NOx	CO	HC	CO_2	O_2	Smoke
1	0.93	0.38	0.42	0.00	0.94	0.77	0.07	0.93	0.02	0.00
2	0.41	0.38	0.58	0.31	0.52	0.79	0.26	0.84	0.05	0.61
3	0.19	0.24	0.39	0.53	0.27	0.60	0.50	0.82	0.05	0.92
4	0.04	0.08	0.11	0.67	0.14	0.78	0.37	0.76	0.09	0.57
5	0.21	0.02	0.06	0.51	0.37	0.29	0.05	0.65	0.31	0.20
6	0.26	0.08	0.14	0.46	0.47	0.26	0.02	0.64	0.35	0.20
7	0.05	0.00	0.00	0.67	0.15	0.75	0.31	0.82	0.05	0.06
8	0.35	0.52	0.12	1.00	1.46	0.00	1.00	0.00	1.00	0.45
9	0.37	0.38	0.58	0.36	0.48	0.82	0.38	0.83	0.05	0.52
10	0.12	0.18	0.30	0.59	0.22	0.83	0.39	0.75	0.09	0.26
11	0.45	0.38	0.58	0.28	0.51	0.75	0.19	0.81	0.06	0.23
12	0.37	0.18	0.30	0.35	0.51	0.32	0.00	0.62	0.35	0.44
13	0.01	0.08	0.11	0.70	0.03	0.97	0.46	0.83	0.04	0.40
14	0.01	0.00	0.01	0.70	0.15	0.62	0.26	0.72	0.12	0.13
15	0.73	1.00	1.00	0.48	0.71	0.79	0.47	1.00	0.00	0.77
16	0.00	0.00	0.00	0.71	0.05	0.56	0.15	0.69	0.15	0.00
17	1.00	0.48	0.69	0.15	1.00	0.71	0.10	0.92	0.03	0.17
18	0.53	0.38	0.64	0.20	0.72	0.67	0.15	0.77	0.08	0.38
19	0.12	0.18	0.30	0.59	0.09	0.94	0.44	0.85	0.04	0.38
20	0.01	0.08	0.11	0.70	0.00	0.94	0.45	0.81	0.06	0.27
21	0.08	0.18	0.30	0.63	0.21	0.60	0.36	0.87	0.04	0.39
22	0.07	0.08	0.14	0.63	0.33	0.67	0.23	0.70	0.14	0.38
23	0.20	0.02	0.06	0.51	0.35	0.31	0.04	0.47	0.30	0.22
24	0.89	0.52	0.83	0.41	0.89	0.77	0.25	0.93	0.02	1.00
25	0.36	0.38	0.58	0.35	0.29	1.00	0.58	0.99	0.00	0.75

Table 16. GRC and GRG with a rank of B20 blend fuel

	Grey-Relational Coefficients (Distinguishing Coefficient ψ = 0.5)											
Run	**BTE**	**BMEP**	**BP**	**BSFC**	**NOx**	**CO**	**HC**	**CO2**	**O2**	**Smoke**	**GRG**	**Rank**
1	0.348	0.288	0.338	0.288	0.278	0.301	0.394	0.276	0.480	0.459	0.345	22
2	0.433	0.335	0.333	0.486	0.334	0.322	0.381	0.372	0.418	0.342	0.375	13
3	0.488	0.405	0.398	0.373	0.383	0.282	0.275	0.305	0.470	0.356	0.374	14
4	0.495	0.456	0.458	0.364	0.403	0.303	0.293	0.341	0.444	0.412	0.397	9
5	0.477	0.487	0.482	0.389	0.409	0.423	0.393	0.442	0.350	0.470	0.432	2
6	0.457	0.456	0.445	0.425	0.362	0.500	0.500	0.500	0.250	0.421	0.432	3
7	0.498	0.500	0.500	0.360	0.487	0.324	0.335	0.395	0.407	0.500	0.431	4
8	0.301	0.269	0.283	0.250	0.266	0.325	0.368	0.276	0.478	0.335	0.315	24
9	0.453	0.335	0.333	0.434	0.357	0.294	0.288	0.316	0.460	0.314	0.358	20
10	0.488	0.405	0.398	0.373	0.411	0.286	0.264	0.348	0.441	0.401	0.381	11
11	0.435	0.335	0.333	0.486	0.288	0.321	0.384	0.360	0.425	0.335	0.370	16
12	0.458	0.405	0.398	0.425	0.337	0.383	0.404	0.462	0.340	0.317	0.393	10
13	0.490	0.441	0.439	0.373	0.450	0.263	0.253	0.291	0.474	0.329	0.380	12
14	0.493	0.500	0.494	0.367	0.430	0.359	0.341	0.412	0.389	0.407	0.419	5
15	0.326	0.250	0.302	0.327	0.290	0.303	0.284	0.276	0.484	0.288	0.313	25
16	0.483	0.500	0.500	0.379	0.392	0.431	0.439	0.453	0.340	0.473	0.439	1
17	0.250	0.443	0.374	0.278	0.260	0.329	0.424	0.309	0.459	0.371	0.350	21
18	0.429	0.335	0.323	0.500	0.286	0.347	0.401	0.392	0.403	0.307	0.372	15
19	0.471	0.383	0.376	0.401	0.390	0.250	0.250	0.250	0.500	0.358	0.363	18
20	0.500	0.456	0.458	0.357	0.500	0.276	0.266	0.351	0.440	0.368	0.397	8
21	0.478	0.405	0.398	0.389	0.393	0.282	0.293	0.298	0.473	0.288	0.370	17
22	0.491	0.456	0.445	0.370	0.383	0.332	0.353	0.417	0.387	0.353	0.399	7
23	0.474	0.487	0.476	0.398	0.392	0.444	0.437	0.473	0.315	0.256	0.415	6
24	0.379	0.358	0.250	0.412	0.250	0.298	0.294	0.263	0.492	0.250	0.325	23
25	0.455	0.335	0.333	0.434	0.374	0.270	0.277	0.263	0.494	0.356	0.359	19

Table 17. GRC and GRG with rank of B30 blend fuel

	Grey-Relational Coefficients (Distinguishing Coefficient ψ = 0.5)											
Run	**BTE**	**BMEP**	**BP**	**BSFC**	**NOx**	**CO**	**HC**	**CO2**	**O2**	**Smoke**	**GRG**	**Rank**
1	0.26	0.36	0.35	0.50	0.21	0.28	0.47	0.26	0.49	0.50	0.37	12
2	0.35	0.36	0.32	0.38	0.25	0.28	0.40	0.27	0.48	0.31	0.34	21
3	0.42	0.40	0.36	0.33	0.29	0.31	0.33	0.27	0.48	0.26	0.35	18
4	0.48	0.46	0.45	0.30	0.31	0.28	0.36	0.28	0.46	0.32	0.37	10
5	0.41	0.49	0.47	0.33	0.27	0.39	0.48	0.30	0.38	0.42	0.39	5
6	0.40	0.46	0.44	0.34	0.26	0.40	0.49	0.30	0.37	0.42	0.39	6
7	0.48	0.50	0.50	0.30	0.31	0.29	0.38	0.27	0.48	0.47	0.40	4
8	0.37	0.33	0.45	0.25	0.17	0.50	0.25	0.50	0.25	0.35	0.34	20
9	0.37	0.36	0.32	0.37	0.26	0.27	0.36	0.27	0.48	0.33	0.34	22
10	0.45	0.42	0.39	0.31	0.30	0.27	0.36	0.29	0.46	0.40	0.36	14
11	0.34	0.36	0.32	0.39	0.25	0.28	0.42	0.28	0.47	0.41	0.35	16
12	0.37	0.42	0.39	0.37	0.25	0.38	0.50	0.31	0.37	0.35	0.37	11
13	0.49	0.46	0.45	0.29	0.34	0.25	0.34	0.27	0.48	0.36	0.38	9
14	0.49	0.50	0.49	0.29	0.31	0.31	0.40	0.29	0.45	0.44	0.40	3
15	0.29	0.25	0.25	0.34	0.23	0.28	0.34	0.25	0.50	0.28	0.30	25
16	0.50	0.50	0.50	0.29	0.33	0.32	0.43	0.30	0.43	0.50	0.41	1
17	0.25	0.34	0.30	0.43	0.20	0.29	0.45	0.26	0.49	0.43	0.34	19
18	0.33	0.36	0.31	0.42	0.23	0.30	0.43	0.28	0.46	0.36	0.35	17
19	0.45	0.42	0.39	0.31	0.32	0.26	0.35	0.27	0.48	0.36	0.36	15
20	0.49	0.46	0.45	0.29	0.34	0.26	0.34	0.28	0.47	0.39	0.38	7
21	0.46	0.42	0.39	0.31	0.30	0.31	0.37	0.27	0.48	0.36	0.37	13
22	0.47	0.46	0.44	0.31	0.28	0.30	0.41	0.29	0.44	0.36	0.38	8
23	0.42	0.49	0.47	0.33	0.28	0.38	0.48	0.34	0.38	0.41	0.40	2
24	0.26	0.33	0.27	0.35	0.21	0.28	0.40	0.26	0.49	0.25	0.31	24
25	0.37	0.36	0.32	0.37	0.29	0.25	0.32	0.25	0.50	0.29	0.33	23

Table 18. Analysis of variance of B20 blend fuel

Source	DF	Seq SS	Contribution (%)	Adj SS	Adj MS	F-Value	P-Value
CR	4	0.001788	5.83	0.001788	0.000447	3.05	0.153
IP (MPa)	4	0.000079	0.26	0.000079	0.000020	0.13	0.961
IT (0b TDC)	4	0.000384	1.25	0.000384	0.000096	0.65	0.655
Load (%)	4	0.026987	87.90	0.026987	0.006747	45.99	0.001
EGR (%)	4	0.000877	2.86	0.000877	0.000219	1.49	0.353
Error	4	0.000587	1.91	0.000587	0.000147		
Total	24	0.030702	100.00				

Table 19. Analysis of variance of B30 blend fuel

Source	DF	Seq SS	Contribution (%)	Adj SS	Adj MS	F-Value	P-Value
CR	4	0.001729	9.40	0.001729	0.000432	3.60	0.121
IP (MPa)	4	0.000620	3.37	0.000620	0.000155	1.29	0.406
IT (0b TDC)	4	0.000558	3.04	0.000558	0.000140	1.16	0.444
Load (%)	4	0.014478	78.73	0.014478	0.003619	30.12	0.003
EGR (%)	4	0.000524	2.85	0.000524	0.000131	1.09	0.468
Error	4	0.000481	2.61	0.000481	0.000120		
Total	24	0.018390	100.00				

3.5.1.5. Nox emissions

NOx emissions occur when a vehicle's exhaust releases nitrogen oxides. Figure 8e shows that B20CV + 100 ppm ZnO produces higher NOx emissions than standard diesel. The higher oxygen content of biodiesel, which leads to more complete combustion and higher peak temperatures, which increase NOx formation.

3.5.1.6. CO emissions

CO is a toxic byproduct of incomplete combustion. Figure 8f shows that B20CV with 100 ppm ZnO produces higher CO emissions than regular diesel. This may be due to the tendency of ZnO nanoparticles to agglomerate, reducing catalytic efficiency and causing incomplete combustion.

3.5.1.7. HC emissions

Figure 8g shows that B20CV + 100 ppm ZnO produces higher unburnt hydrocarbon (HC) emissions than standard diesel. This may be due to localized areas of incomplete combustion caused by ZnO nanoparticle agglomeration.

3.5.1.8. CO2 emissions

CO2 is produced by complete combustion. Figure 8h shows that B20CV + 100 ppm ZnO emits more CO2 than regular diesel. Biodiesel has a higher fatty acid content, and ZnO nanoparticles increase combustion efficiency.

3.5.1.9. O2 emissions

Figure 8i shows that B20CV + 100 ppm ZnO produces lower O2 emissions than standard diesel. This is due to the higher oxygen content in biodiesel and the catalytic effect of ZnO, both of which lead to more complete combustion.

3.5.1.10. Smoke emissions

Smoke emissions, primarily resulting from incomplete combustion, are lower with B20CV + 100 ppm ZnO than with standard diesel, as shown in Figure 8j. This is likely due to the higher oxygen content of biodiesel, which reduces soot formation.

3.5.2. Comparison of B30CV algae biodiesel against standard diesel

3.5.2.1. Brake thermal efficiency (BTE)

Figure 9a indicates that B30CV + 100ppm ZnO exhibits a lower BTE than standard diesel. This reduction is attributed to the lower calorific value of biodiesel and to the use of exhaust gas recirculation (EGR), the latter which reduces NOx emissions but also decreases combustion efficiency

3.5.2.2. Brake power (BP)

As shown in Figure 9b, the brake power of B30CV + 100ppm ZnO is lower than that of standard diesel. This outcome results from agglomeration of ZnO nanoparticles and biodiesel's higher viscosity, which impair fuel atomization and lead to incomplete combustion.

3.5.2.3. Brake mean effective pressure (BMEP)

Figure 9c demonstrates that B30CV + 100ppm ZnO results in lower BMEP than standard diesel. The reduction in BMEP results from slower combustion and increased heat transfer to the cylinder walls both of which diminish energy conversion efficiency.

3.5.2.4. Brake specific fuel consumption (BSFC)

Figure 9d shows that B30CV + 100ppm ZnO has a higher BSFC than standard diesel. The lower combustion temperature and lower calorific value of biodiesel require more fuel to achieve the same power output, thereby reducing overall fuel efficiency.

3.5.2.5. NOx emissions

Figure 9e shows that the NOx emissions are lower for B30CV + 100ppm ZnO than that of standard diesel. The catalytic effect of ZnO nanoparticles helps in combustion at lower temperatures, which reduces the formation of NOx.

3.5.2.6. CO emissions

Figure 9f shows that CO emissions of B30CV + 100ppm ZnO are greater than standard diesel. The Increase may be due to agglomeration of ZnO nanoparticles which inhibit catalytic activity, incomplete combustion.

3.5.2.7. HC emissions

As shown in Figure 9g, B30CV + 100ppm ZnO has higher HC emissions than diesel. The incomplete combustion and higher hydrocarbon emissions are due to the uneven distribution of oxygen in the fuel.

3.5.2.8. CO2 emissions

As shown in Figure 9h, B30CV + 100ppm ZnO exhibits higher CO2 emissions. Although some localized regions of incomplete combustion are seen, the overall combustion process is more efficient owing to the long chain fatty acids and the catalytic effect of ZnO nanoparticles.

3.5.2.9. O2 emissions

Figure 9i shows that the O2 emission of B30CV + 100ppm ZnO is lower than that of the standard diesel. This means that the oxygen content of biodiesel leads to more complete combustion.

3.5.2.10. Smoke emissions

Figure 9j demonstrates that B30CV + 100ppm ZnO results in lower smoke emissions than standard diesel. The reduced smoke is attributed to the higher oxygen content and more complete combustion associated with biodiesel.

3.5.3. Comparison of ANN and experimental results

The experimental results obtained from running the engine on B20CV + 100ppm ZnO and B30CV + 100ppm ZnO were close to values predicted by ANN modelling. From Figures 10 and 11, it is seen that the performance and emission parameters such as BTE, BMEP, BP, BSFC, CO, HC, CO2, O2 and Smoke are in close agreement with experimental(actual) results, showing the accuracy of the ANN model in predicting the parameters. But there is a considerable difference in the NOx emission level as reported in Figures 10e and 11e. The high correlation coefficient between experimental and ANN-predicted results for these parameters shows that the ANN model can capture the characteristics of the biodiesel blends. This therefore confirms its effectiveness for engine performance modelling. On the contrary, the discrepancy in NO_x emission suggests that the ANN model has not been able to fully capture the complex contrivance involved in NO_x formation under varying operating conditions. This could be mostly attributed to the inherent variability in the experimental setup and the sensitivity of NO_x formation to minor changes in combustion conditions. Table 20 presents the confirmation test results for B20CV+100 ppm ZnO. All three experiments were conducted under identical operating conditions: compression ratio (CR) of 14, injection pressure (IP) of 200 bar, injection timing (IT) of 21° before TDC, load of 100%, and exhaust gas recirculation (EGR) of 12%. The first column of Table 20 presents the Artificial Neural Network (ANN) predictions of emission and performance parameters. The second column shows experimental results for the B20CV+100 ppm ZnO blend, and the third column shows results for conventional diesel.

Table 21 presents the confirmation test results for B30CV+100 ppm ZnO. All three experiments were conducted under identical operating conditions: compression ratio (CR) of 14 injection pressure (IP) of 200 bar, injection timing (IT) of 17°before top dead center (BTDC), load of 100%, and exhaust gas recirculation (EGR) of 9%. The first column of Table 21 presents the Artificial Neural Network (ANN) predictions of emission and performance parameters. The second column presents the experimental results obtained with the B30CV+100 ppm ZnO blend, while the third presents the results for conventional diesel.

Table 20. Confirmation test for B20CV+100 ppm ZnO fuel

Fuel and Experiment Type	BTE (%)	BMEP (bar)	BP (KW)	BSFC	NOx (ppm vol)	CO (% vol)	HC (ppm vol hex)	CO_2 (% vol)	O_2 (% vol)	Smoke
B20CV+100 ppm ZnO ANN	15.30	3.31	2.98	0.45	144.72	2.39	297.59	9.05	6.06	23.96
B20CV+100 ppm ZnO Experimental	21.2	4.1	3.3	0.41	75	3.1	221	9	5.81	20.7
Diesel Experimental	21	4.1	3.2	0.42	44	1.98	130	5.9	11.2	28.1

Table 21. Confirmation test for B30CV+100 ppm ZnO fuel

Fuel and Experiment Type	BTE (%)	BMEP (bar)	BP (KW)	BSFC	NOx (ppm vol)	CO (% vol)	HC (ppm vol hex)	CO_2 (% vol)	O_2 (% vol)	Smoke
B30CV+100 ppm ZnO ANN	14.40	1.95	2.61	0.24	56.12	1.68	223.62	7.21	9.95	27.38
B30CV+100 ppm ZnO Experimental	20.10	3.80	3.10	0.44	125.00	1.87	155.00	9.70	6.30	23.50
Diesel Experimental	23.70	4.10	3.40	0.36	127.00	1.62	148.00	9.00	7.29	127.00

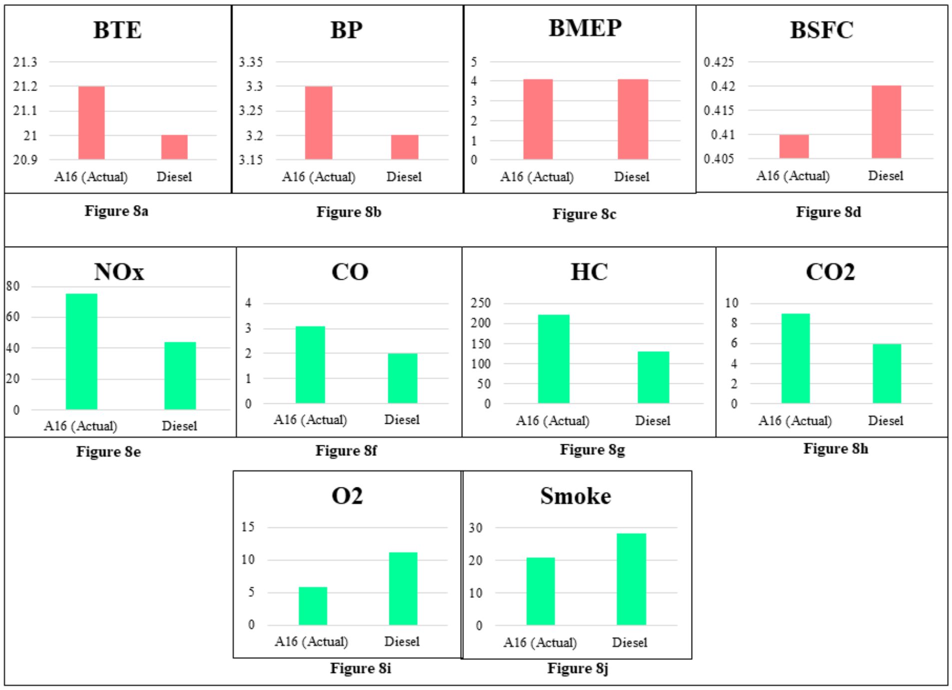

Figure 8. Comparative analysis of engine performance and emission characteristics for B20CV + 100 ppm ZnO blend versus standard diesel

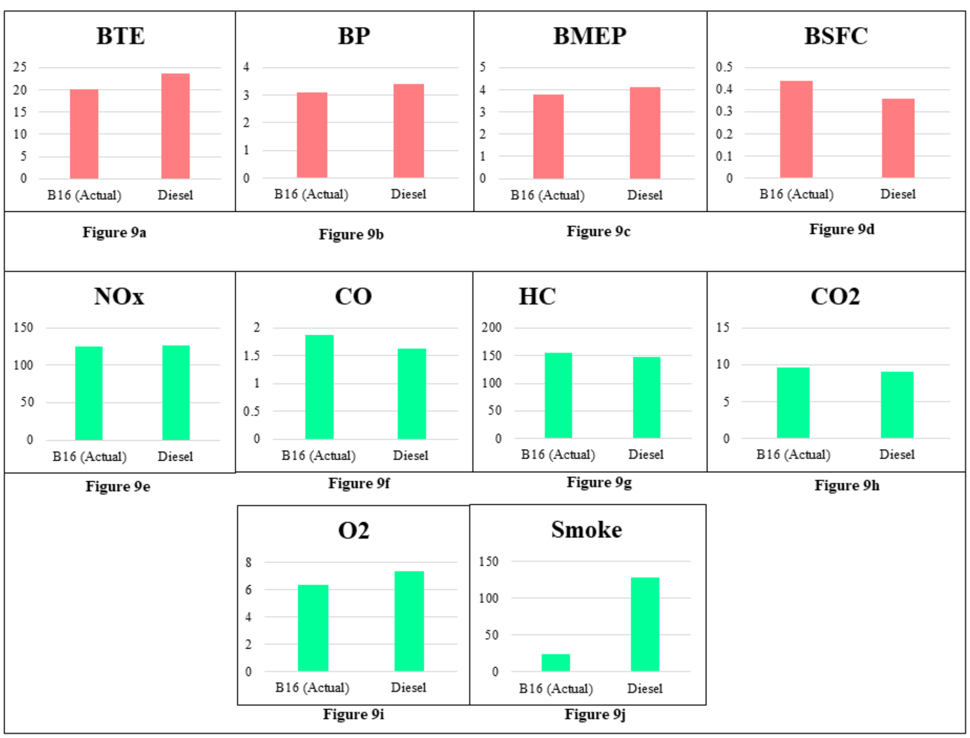

Figure 9. Comparative analysis of engine performance and emission characteristics for B30CV + 100ppm ZnO blend versus standard diesel

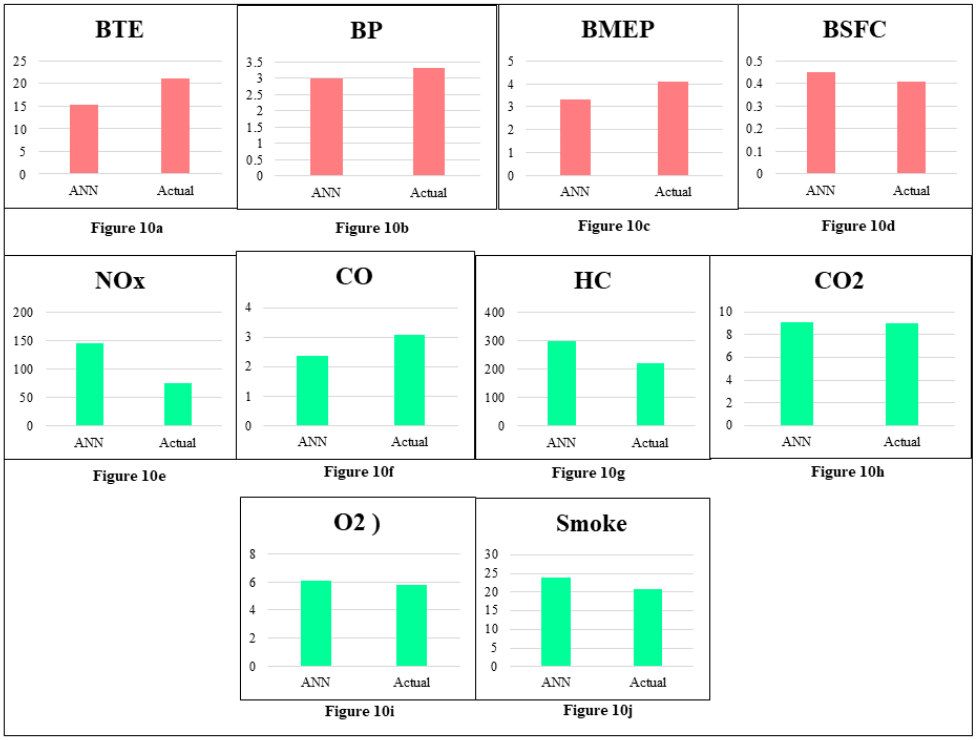

Figure 10. Comparison between predicted ANN outputs and experimental results for B20 blend across performance and emission parameters

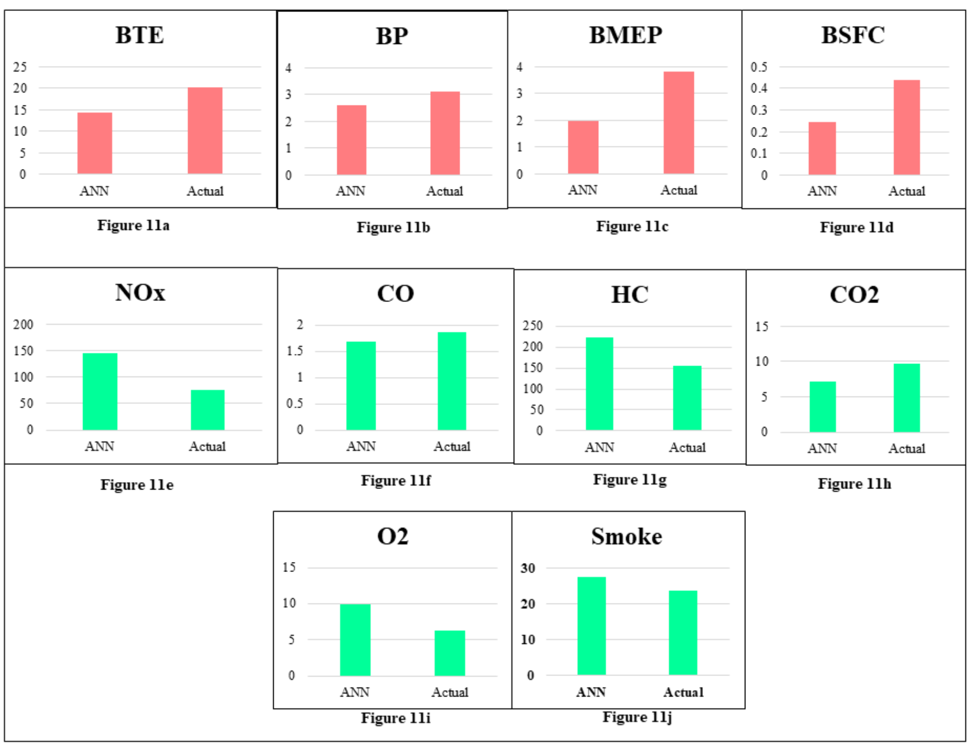

Figure 11. Comparison between predicted ANN outputs and experimental results for B30 blend across performance and emission parameters

3.6. Uncertainty analysis

Statistical analysis of uncertainty is a critical part of experimental research, as the instruments used to measure a variety of parameters are susceptible to random errors influenced by factors such as equipment conditions, laboratory calibration, environmental variables, and measurement readings. Consequently, we employ a mathematical method, known as the propagation of errors, to reduce the likelihood of errors. The uncertainties in parameter values estimated by instruments can be attributed to equipment errors during experiments. The overall percentage uncertainty is decided using Equation (8). The engine's overall performance and emissions profile are influenced by each parameter in the equation. The reliability of the experimental results is influenced by the uncertainty of each parameter, which reflects the potential variability or measurement error.

Tables 22 and 23 give the comparison of the present study results with earlier findings. Based on the comparative analysis of performance and emission parameters presented in Tables 22 and 23, the study highlights both the advantages and limitations of biodiesel blends with ZnO nanoparticle additives. In terms of performance, earlier studies such as Satputaley et al. (2018) and Mathimani et al. (2017) reported a reduction in Brake Thermal Efficiency (BTE) for biodiesel and algae oil, with decreases of approximately 5.2% and 6.4%, respectively, compared to diesel. However, in the present study, the B20 blend enriched with 100 ppm ZnO nanoparticles achieved a marginal increase in BTE to 21.2% compared to 21% for diesel. Conversely, a higher blend ratio (B30 + 100 ppm ZnO) led to a reduction in BTE to 20.1% versus 23.7% for diesel, showing that while ZnO enhances performance at lower blend levels, its effect diminishes at higher concentrations. About Brake brake-specific fuel Consumption (BSFC), biodiesel typically consumes more fuel for equivalent power output, as noted by Satputaley et al. (2018). Yet, the B20 + 100 ppm ZnO blend showed an improved BSFC (0.41 kg/kWh) over standard diesel (0.42 kg/kWh), while the B30 + ZnO blend proved a higher BSFC (0.44 kg/kWh) than diesel (0.36 kg/kWh), reaffirming the benefits of best nanoparticle dosing.

Study results on emissions are mixed. Oxygen and hydrogen enrichment reduced CO and HC emissions (Satputaley et al., 2018; Tayari, 2019). The biodiesel-ZnO blends had higher CO emissions than diesel (1.62% Vol) (3.1% Vol for B20CV and 1.87% Vol for B30CV). B20CV and B30CV had 221 ppm and 155 ppm HC emissions, higher than diesel (148 ppm), but nanoparticle addition reduced emissions from unmodified blends. Smoke emissions improved significantly with B30CV and B20CV at 23.5 mg/m³ and 20.7 mg/m³, respectively, compared to diesel at 127 mg/m³ and 28.1 mg/m³, indicating ZnO's particulate suppression effect. Moderate mitigation was also seen in NOx emissions, with the B20CV blend emitting 125 ppm, which is slightly below diesel emissions of 127 ppm. Overall, ZnO nanoparticles have a good effect in the improvement of combustion efficiency and decrease of particulate emissions, but their effect on gaseous emissions such as CO and HC is limited, particularly at higher blends.

Table 22. Comparison of present study with earlier findings (performance parameter)

Performance Parameters	Results	Reference
BTE	Biodiesel and Algae Oil show a reduction in BTE of about 5.2% and 6.4% compared to diesel.	Satputaley et al. (2018)
	BTE diminished with an increase in blends.	Mathimani et al. (2017)
	The biodiesel blend B20 + 100 ppm ZnO exhibited an increase in brake thermal efficiency (BTE) (21.2%) compared to standard diesel (21%) at full load. Conversely, the B30 + 100 ppm ZnO blend proved a reduction in BTE (20.1%), in contrast to standard diesel (23.7%)	**Present Study**
BSFC	Biodiesel and Algae Oil consume more fuel to give the same power output.	Satputaley et al. (2018)
	BSFC improved by 6.6% with 10 LPM hydrogen gas for the blend B20.	Tayari et al. (2019)
	The biodiesel blend B20 + 100 ppm ZnO exhibited a reduction in brake-specific fuel consumption (BSFC) (0.41 kg/kWh) compared to standard diesel (0.42 kg/kWh) at full load. In contrast, the B30 + 100 ppm ZnO blend proved an increase in BSFC (0.44 kg/kWh) compared to standard diesel (0.36 kg/kWh).	**Present Study**

Table 23. Comparison of present study with earlier findings (emission parameter)

Emission Parameters	Results	Reference
CO	10 to 12% excess oxygen level in methyl ester and algae oil results in reduced CO emissions.	Satputaley et al. (2018)
	CO emissions are reduced by 13.7% because of hydrogen enrichment.	Tayari et al. (2019)
	The B20CV + 100 ppm ZnO blend exhibited CO emissions of 3.1% Vol at full load, while the B30CV + 100 ppm ZnO blend recorded 1.87% Vol. However, both blends proved higher CO emissions compared to standard diesel (1.62% Vol)	**Present Study**
HC	10 to 12% excess oxygen level in methyl ester and algae oil results in reduced UHC emissions.	Satputaley et al. (2018)
	HC emissions are reduced by 34.3% because of hydrogen enrichment.	Tayari et al. (2019)
	The addition of ZnO nanoparticles led to a reduction in HC emissions, with values of 221 ppm for B20CV + 100 ppm ZnO and 155 ppm for B30CV + 100 ppm ZnO. However, HC emissions for both blends remained higher compared to standard diesel (148 ppm)	**Present Study**
Smoke	10 to 12% excess oxygen level in methyl ester and algae oil results in reduced Smoke Opacity.	Satputaley et al. (2018)
	The addition of 100 ppm ZnO nanoparticles resulted in a significant reduction in smoke emissions, with values of 23.5 mg/m³ for B30CV + 100 ppm ZnO, compared to 127 mg/m³ for standard diesel at full load. Similarly, the B20CV + 100 ppm ZnO blend showed lower smoke emissions (20.7 mg/m³) than standard diesel (28.1 mg/m³)	**Present Study**
NO_x	At 5.15 kW power load, algae oil proved the greatest reduction in NO_x of 19 ppm.	Satputaley et al. (2018)
	NO_x emissions were reduced by 5.1% when hydrogen was enriched.	Tayari et al. (2019)
	The B20CV + 100 ppm ZnO blend exhibited NO_x emissions of 125 ppm at full load, which was slightly lower than standard diesel (127 ppm) under the same conditions.	**Present Study**

4. Conclusion

Algae oil is a significant feedstock for biodiesel production because it is consumed at high levels both nationally and globally. Biodiesel derived from algae oil is considered a third-generation renewable fuel that does not compromise food security. The performance and emission characteristics of Cholera Vulgaris biodiesel blend with Al_2O_3 and ZnO were investigated on a single-cylinder, four-stroke diesel engine with VCR and various optimization techniques were used to interpret the results. Nanomaterials improve combustion characteristics by enhancing fuel atomization, catalytic activity, and thermal conductivity. Air and fuel mix better with more surface area, improving combustion efficiency and reducing emissions. ZnO and Al_2O_3 nanoparticles impact fuel viscosity and density, affecting injection characteristics, spray formation, engine performance, and emissions. ANN models were also created to test performance and emission predictions. Nano-additives improve biodiesel performance but can cause instability, injector clogging, and high costs. Agglomeration clogs filters and reduces engine life. Despite these limitations, the results will help perfect biodiesel-nanoparticle blends to improve engine performance and control emissions without engine modifications. The novelty of this work is underscored by its integration of optimization techniques and predictive modeling to assess the feasibility of algae-based nano-biodiesel blends in improving CI engine performance and reducing emissions.

The following conclusions were the most notable and were drawn from the experiment conducted:

- For B20CV + 100ppm ZnO, performance characteristics such as BTE, BP, and BSFC improved compared to standard diesel, while BMEP stayed the same. Such equality from similar energy densities in biodiesel and standard diesel.

On the contrary, the results obtained for emission characteristics such as NO_x, CO, HC, and CO_2 were found to be discrepancies. The most conspicuous reason for such anomalies could be the agglomeration of ZnO nanoparticles which causes localized regions of incomplete combustion.

In the case of B30CV + 100ppm ZnO, opposite results were obtained for the performance parameters. BTE, BP, and BMEP were lower than those of standard diesel while BSFC was higher. This could be due to an increase in the percentage of biodiesel in the fuel which causes a significant reduction in the lower calorific value, resulting in lower energy content.

The emissions parameters, however, such as NO_X, O_2 and smoke were better than their diesel counterpart. In contrast, CO and HC were anomalies resulting from inconsistent atmospheric conditions in the experimental setup and other random errors.

The ANN model, which was created using MATLAB R2024a (24.1) for both B20CV and B30CV, was found to confirm its definition. The performance and emission characteristics in the experimental and ANN results were highly correct. However, the NO_x emission results were found to be less correlated. This is because the model could not grab the sensitivity of NO_x formation to minor changes in combustion conditions.

Acknowledgement

The authors would like to thank Symbiosis Skills and Professional University, Pune, India for providing support in research work and preparation of this manuscript

Authorship contributions

Sumit Dubal: Conceptualization, Investigation, Formal analysis, Writing original draft; Aryaman Salaria: Experimentation work, Data Curation. Sahaj Joshi: Experimentation work, Data Curation.

Data availability statement

The authors confirm that the data that supports the findings of this study are available within the article. Raw data that support the finding of this study are available from the corresponding author, upon reasonable request.

Conflict of interest

The authors declare that they have no competing interests.

Statement on the use of Artificial Intelligence

No generative AI or AI-assisted technologies were used in the preparation of this manuscript.

Nomenclature

CV	Chlorella Vulgaris
HC	Hydrocarbons
CO	Carbon Monoxide
CI	Compression ignition
O2	Oxygen
NOx	Nitrogen oxides
CO2	Carbon dioxide
BTE	Brake Thermal Efficiency
BSFC	Brake Specific Fuel Consumption
BMEP	Brake Mean Effective Pressure
BP	Brake Power
ANN	Artificial Neural Network
Al_2O_3	Aluminium Oxide
ZnO	Zinc Oxide

References

[1] A. Kumar, S. Luthra, S.K. Mangla, J.A. Garza-Reyes, Y. Kazancoglu, Analysing the adoption barriers of low-carbon operations: A step forward for achieving net-zero emissions, Resour. Policy 80(2023)103256. https://doi.org/10.1016/j.resourpol.2022.103256.

[2] T. Subhaschandra Singh, T. Nath Verma, P. Nashine, Analysis of an Anaerobic Digester using Numerical and Experimental Method for Biogas Production, Mater. Today Proc. 5(2018)5202–5207. https://doi.org/10.1016/j.matpr.2017.12.102.

[3] B. Mohamad, G.L. Szepesi, B. Bollo, Review Article: Effect of Ethanol-Gasoline Fuel Blends on the Exhaust Emissions and Characteristics of SI Engines, in: K. Jármai, B. Bolló (Eds.), Veh. Automot. Eng. 2, Springer International Publishing, Cham, 2018: pp. 29–41. https://doi.org/10.1007/978-3-319-75677-6_3.

[4] S. Mathur, H. Waswani, D. Singh, R. Ranjan, Alternative Fuels for Agriculture Sustainability: Carbon Footprint and Economic Feasibility, AgriEngineering 4 (2022) 993–1015. https://doi.org/10.3390/agriengineering4040063.

[5] A. Kolakoti, OPTIMIZATION OF BIODIESEL PRODUCTION FROM WASTE COOKING SUNFLOWER OIL BY TAGUCHI AND ANN TECHNIQUES, J. Therm. Eng. 6(2020)712–723. https://doi.org/10.18186/thermal.796761.

[6] A. Ahmadbeigi, Biodiesel production from waste cooking oil: A review on production methods, recycling models, materials and catalysts, J. Therm. Eng. (2024)1362–1389. https://doi.org/10.14744/thermal.0000826.

[7] T. Kajale, A. Pawar, J. Hole, S. Dubal, Selection of Optimal Waste Cooking Soybean Oil Biodiesel Blends for Emission Reduction in CI Diesel Engines Under Variable Loads: A Combined Analytic Hierarchy Process (AHP)-Technique for Order of Preference by Similarity to Ideal Solution (TOPSIS) Analysis, Int. J. Automot. Sci. Technol. 8 (2024) 457–466. https://doi.org/10.30939/ijastech.1550536.

[8] [8]T. Kajale, J. Hole, A. Pawar, S. Dubal, Optimizing Performance and Emissions of VCR Diesel Engines Using Grey-Taguchi Methods and ANN with Biodiesel from Waste Cooking Soybean Oil, Int. J. Heat Technol. 43(2025)228–240. https://doi.org/10.18280/ijht.430124.

[9] S.N. Naik, V.V. Goud, P.K. Rout, A.K. Dalai, Production of first and second generation biofuels: A comprehensive review, Renew. Sustain. Energy Rev. 14 (2010) 578–597. https://doi.org/10.1016/j.rser.2009.10.003.

[10] B.N. Kale, S.D. Patle, State of art review of algal biodiesel and its blends influence on performance and emission characteristics of compression ignition engine, Clean. Eng. Technol. 7(2022)100431. https://doi.org/10.1016/j.clet.2022.100431.

[11] P. Nautiyal, K.A. Subramanian, M.G. Dastidar, Kinetic and thermodynamic studies on biodiesel production from Spirulina platensis algae biomass using single stage extraction–transesterification process, Fuel 135(2014)228–234. https://doi.org/10.1016/j.fuel.2014.06.063.

[12] V. Carolina Vieira, I. Hachemi, S.P. Freitas, P. Mäki-Arvela, A. Aho, J. Hemming, A. Smeds, I. Heinmaa, F.B. Fontes, D.C. Da Silva Pereira, N. Kumar, D.A.G. Aranda, D.Yu. Murzin, A route to produce renewable diesel from algae: Synthesis and characterization of biodiesel via in situ transesterification of Chlorella alga and its catalytic deoxygenation to renewable diesel, Fuel 155(2015)144–154. https://doi.org/10.1016/j.fuel.2015.03.064.

[13] S. Dubal, S. Chavan, G. Lohar, P. Lokhande, U. Rednam, D. Kumar, Polyacrylonitrile-based carbon nanofiber electrode fabricated via electrospun for supercapacitor application, Proc. Inst. Mech. Eng. Part N J. Nanomater. Nanoeng. Nanosyst.(2024)23977914241232161. https://doi.org/10.1177/23977914241232161.

[14] S. Dubal, S. Chavan, P. Jadhav, S. Kadam, S. Dhotre, Effects of stabilization on structures and properties of Electrospun Polyacrylonitrile based carbon nanofibers as a binder free electrode for supercapacitor application, Mater. Today Proc. (2022) S2214785322048726. https://doi.org/10.1016/j.matpr.2022.07.250.

[15] S. Dubal, S. Chavan, P. Jadhav, Oxidative Stabilization and Characterization of Electrospun Polyacrylonitrile Nanofiber Web on Different Substrates, J. Inst. Eng. India Ser. C (2022) 1–8. https://doi.org/10.1007/s40032-022-00874-0.

[16] S. Chavan, S. Dubal, Nanotechnology Applications In Automobiles: Comprehensive Review Of Existing Data, 7 (2020) 18–22.

[17] D.D. Mohite, S.S. Chavan, P.E. Lokhande, S. Dubal, V. Kadam, C. Jagtap, U. Rednam, M. Salve, N.B. Chaure, B.A. Al-Asbahi, Y.A. Kumar, Electrochemical characterization of electrospun Co3O4/PAN-based carbon nanofiber composites for supercapacitor applications, J. Mater. Sci. 59 (2024) 11440–11453. https://doi.org/10.1007/s10853-024-09852-6.

[18] S. Dubal, S. Chavan, Electrospun Polyacrylonitrile Carbon Nanofiber for Supercapacitor Application: A Review, Adv. Eng. Forum 40 (2021) 25–42. https://doi.org/10.4028/www.scientific.net/AEF.40.25.

[19] U. Rajak, P. Nashine, P. Kumar Chaurasiya, T. Nath Verma, A numerical investigation of the species transport approach for modeling of gaseous combustion, J. Therm. Eng. 7 (2021) 2054–2067. https://doi.org/10.18186/thermal.1051312.

[20] U. Rajak, M. Panchal, K. Viswanath Allamraju, P. Nashine, T. Nath Verma, A. Pugazhendhi, A numerical investigation on a diesel engine characteristic fuelled using 3D CFD approach, Fuel 368(2024)131488. https://doi.org/10.1016/j.fuel.2024.131488.

[21] P. Shrivastava, U. Rajak, P. Nashine, T.N. Verma, Performance and Emission Characteristics of a Compression Ignition Engine Fueled With Roselle and Karanja Biodiesel, in: Roselle, Elsevier, 2021: pp. 165–176. https://doi.org/10.1016/B978-0-323-85213-5.00015-9.

[22] M. Subbulakshmi, S. Srujana, ArifSenolSener, M.A. Al Zubi, R. Kumar, S. Natarajan, T.D. Gidebo, Environmental Effect of Zinc Oxide Metal Nano Additives in Microalgae Biodiesel in Diesel Engine, J. Nanomater. 2023(2023)1–6. https://doi.org/10.1155/2023/1051117.

[23] M. Singh, S.S. Sandhu, Performance, emission and combustion characteristics of multi-cylinder CRDI engine fueled with argemone biodiesel/diesel blends, Fuel 265 (2020) 117024. https://doi.org/10.1016/j.fuel.2020.117024.

[24] A. Praveen, V. Lakshmi Narayana, K. Ramanaiah, Influence of nanoadditive Chlorella vulgaris microalgae biodiesel blends on the performance and emission characteristics of a DI diesel engine, Int. J. Ambient Energy 43 (2022) 2071–2077. https://doi.org/10.1080/01430750.2020.1725120.

[25] R. Karthikeyan, K. Venkateswarlu, S. Yousufuddin, A. Punitha, Regression and Taguchi – gray analysis for multi response optimization of alternative fuel operated diesel engine with EGR, Energy Sources Part Recovery Util. Environ. Eff. 45 (2023) 11024–11035. https://doi.org/10.1080/15567036.2019.1683101.

[26] E. Ramachandran, R. Krishnaiah, E.P. Venkatesan, M. Murugan, S.R. Medapati, P. Sekar, Experimental Investigation for Determining an Ideal Algal Biodiesel–Diesel Blend to Improve the Performance and Mitigate Emissions Using a Response Surface Methodology, ACS Omega 8(2023)9187–9197. https://doi.org/10.1021/acsomega.2c07104.

[27] M. Gul, A.N. Shah, U. Aziz, N. Husnain, M.A. Mujtaba, T. Kousar, R. Ahmad, M.F. Hanif, Grey-Taguchi and ANN based optimization of a better performing low-emission diesel engine fueled with biodiesel, Energy Sources Part Recovery Util. Environ. Eff. 44 (2022) 1019–1032. https://doi.org/10.1080/15567036.2019.1638995.

[28] A.Z. Hameed, K. Muralidharan, Performance, Emission, and Catalytic Activity Analysis of AL_2 O_3 and CEO_2 Nano-Additives on Diesel Engines Using Mahua Biofuel for a Sustainable Environment, ACS Omega 8 (2023) 5692–5701. https://doi.org/10.1021/acsomega.2c07193.

[29] Y. Kaushik, V. Verma, K.K. Saxena, C. Prakash, L.R. Gupta, S. Dixit, Effect of Al2O3 Nanoparticles on Performance and Emission Characteristics of Diesel Engine Fuelled with Diesel–Neem Biodiesel Blends, Sustainability 14(2022)7913. https://doi.org/10.3390/su14137913.

[30] Z. Guo, Y.-L. Hsieh, S.-L. Lin, Y.-Y. Lee, T.H. Lee, Influence of Renewable Nano-Al_2O_3 on Engine Characteristics and Health Impact under Variable Injection Timings and Excess Air Coefficients, ACS Omega 9 (2024) 49966–49979. https://doi.org/10.1021/acsomega.4c09313.

[31] Bharati Vidyapeeth (Deemed to be University) College of Engineering, Pune-411043, India., M.S. Patil, A.A. Mancharkar, Department of Physics, Modern College of Arts, Science and Commerce, Shivajinagar, Pune- 411005, India., P.. E. Lokhande, Departamento de Ingenieria Mecanica, Facultad de Ingenieria, Universidad Tecnologica Metropolitana, Av. Jose Pedro Alessandri 1242, Santiago 7810003, Chile., S.M. Salunkhe, Bharati Vidyapeeth (Deemed to be University) College of Engineering, Pune-411043, India., Studies on the Electrochemical Performance of Zinc Oxide (ZnO) Thin Film on Different Substrates, ES Mater. Manuf.(2024).https://doi.org/10.30919/esmm1279.

[32] D.D. Mohite, S.S. Chavan, S. Dubal, P.E. Lokhande, V. Kadam, C. Jagtap, U. Rednam, S. Ansar, Y.A. Kumar, Electrochemical evaluation of ZnO and PAN-based carbon nanofibers composite for high-performance supercapacitor application, Ionics 30 (2024) 8469–8480. https://doi.org/10.1007/s11581-024-05869-8.

[33] A. Suhel, N. Abdul Rahim, M.R. Abdul Rahman, K.A. Bin Ahmad, U. Khan, Y.H. Teoh, N. Zainal Abidin, Impact of ZnO nanoparticles as additive on performance and emission characteristics of a diesel engine fueled with waste plastic oil, Heliyon 9 (2023) e14782. https://doi.org/10.1016/j.heliyon.2023.e14782.

[34] S. Gowthaman, A.I. Anu Karthi Swaghatha, K. Thangavel, L. Muthulakshmi, P. Paramasivam, Effect of ZnO nanoparticle on combustion and emission characteristics of a diesel engine powered by lemongrass biodiesel: an experimental approach, Discov. Appl. Sci. 6(2024)344. https://doi.org/10.1007/s42452-024-06045-3.

[35] S.P. Jena, S. Mahapatra, S.K. Acharya, Optimization of performance and emission characteristics of a diesel engine fueled with Karanja biodiesel using Grey-Taguchi method, Mater. Today Proc. 41 (2021) 180–185. https://doi.org/10.1016/j.matpr.2020.08.579.

[36] H.-W. Wu, Z.-Y. Wu, Using Taguchi method on combustion performance of a diesel engine with diesel/biodiesel blend and port-inducting H2, Appl. Energy 104(2013)362–370. https://doi.org/10.1016/j.apenergy.2012.10.055.

[37] Patil Amol Nayakappa, A. Walke Gaurish, Gawkhare Mahesh, Grey Relation Analysis Methodology and its Application, (2019). https://doi.org/10.5281/ZENODO.2578088.

[38] X.H. Wang, C.H. Wan, C.C. Sun, R.W. Xia, An Optimization Algorithm for Multi-objective Optimization Problem by Using Envelope-dual Method, Procedia Eng. 67(2013)457–466. https://doi.org/10.1016/j.proeng.2013.12.046.

[39] G. Pohit, D. Misra, Optimization of Performance and Emission Characteristics of Diesel Engine with Biodiesel Using Grey-Taguchi Method, J. Eng. 2013(2013)915357. https://doi.org/10.1155/2013/915357.

[40] R.M. Dodo, T. Ause, E.T. Dauda, U. Shehu, A.P.I. Popoola, Multi-response optimization of transesterification parameters of mahogany seed oil using grey relational analysis in Taguchi method for quenching application, Heliyon 5 (2019) e02167. https://doi.org/10.1016/j.heliyon.2019.e02167.

[41] R.K. Gupta, A.R. Gupta, N. Pathik, R.K. Pateriya, P.K. Chaurasiya, U. Rakjak, T.N. Verma, A.M. Alosaimi, M.Ali. Hussein, Novel deep neural network technique for detecting environmental effect of COVID-19, Energy Sources Part Recovery Util. Environ. Eff.(2021)1–19. https://doi.org/10.1080/15567036.2021.1941435.

[42] J. Zou, Y. Han, S.-S. So, Overview of Artificial Neural Networks, in: D.J. Livingstone (Ed.), Artif. Neural Netw., Humana Press, Totowa, NJ, 2008: pp. 14–22. https://doi.org/10.1007/978-1-60327-101-1_2.

[43] E. Goz, M. Yuceer, E. Karadurmus, Total Organic Carbon Prediction with Artificial Intelligence Techniques, in: A.A. Kiss, E. Zondervan, R. Lakerveld, L. Özkan (Eds.), Comput. Aided Chem. Eng., Elsevier, 2019: pp. 889–894. https://doi.org/10.1016/B978-0-12-818634-3.50149-1.

[44] P. Achuthamenon Sylajakumari, R. Ramakrishnasamy, G. Palaniappan, Taguchi Grey Relational Analysis for Multi-Response Optimization of Wear in Co-Continuous Composite, Materials 11(2018)1743. https://doi.org/10.3390/ma11091743.

[45] J. Kaufmann, A. Schering, Analysis of Variance ANOVA, in: R.S. Kenett, N.T. Longford, W.W. Piegorsch, F. Ruggeri (Eds.), Wiley StatsRef Stat. Ref. Online, 1st ed., Wiley, 2014. https://doi.org/10.1002/9781118445112.stat06938.

[46] N.B. Shaik, S.R. Pedapati, S.A.A. Taqvi, A.R. Othman, F.A.A. Dzubir, A Feed-Forward Back Propagation Neural Network Approach to Predict the Life Condition of Crude Oil Pipeline, Processes 8(2020)661. https://doi.org/10.3390/pr8060661.